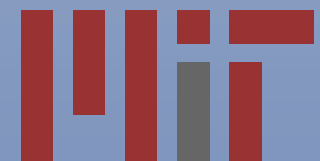


CaF: Just Large Enough, and Ca: Even Smaller

Robert W. Field
Massachusetts Institute of
Technology

12 November 2010



Outline

- Goals
 - Global model: all spectra, all dynamics
 - Core-nonpenetrating states: new state of matter
- Experimental Methods
 - REMPI vs. direct FID detection
- Fits to Massively Perturbed Spectra
 - Multichannel Quantum Defect Theory
- Zone of Death
 - Predissociation and autoionization
- Free Induction Decay Signal: 5 kilo-Debye
 - NMR-esque tricks

Why CaF?

Simplest chemically-relevant “not-atom”

Like Na

1 e^- outside closed-shell ion-core

Unlike Na^+

* $(\text{Ca}^{2+})(\text{F}^-)$ is *profoundly* not round

* Not-roundness is R,E-dependent

Mechanisms for $e^- \leftrightarrow$ nuclei energy exchange

CHEMISTRY!

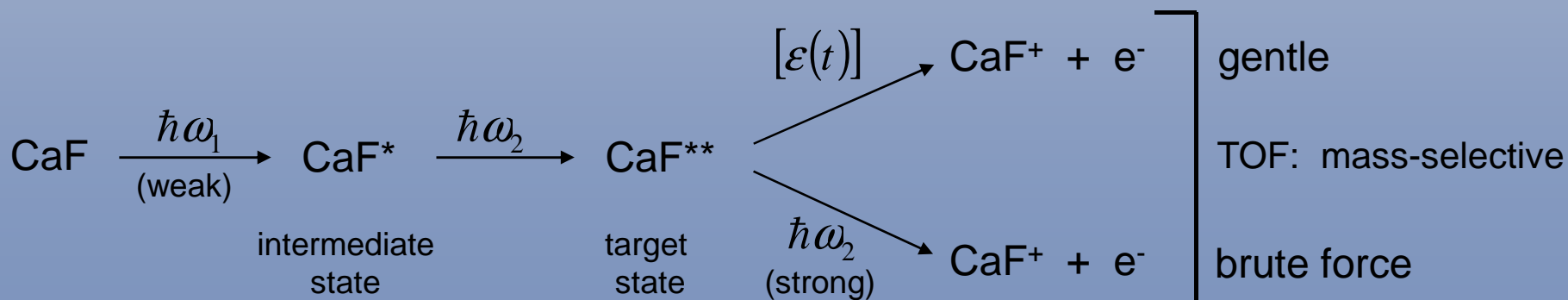
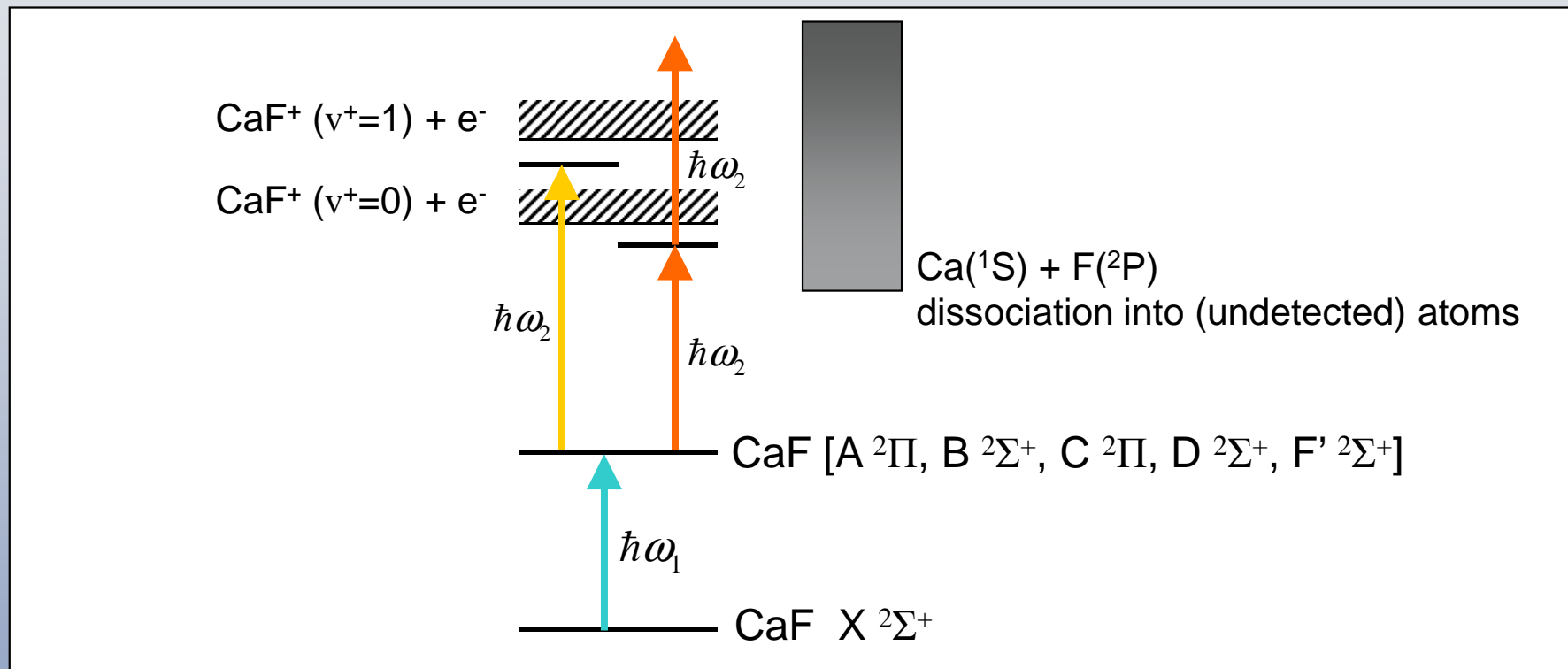
Why Ca?

- Experimentally a little easier than CaF
- Pulsed photo-ablation supersonic jet source, as for CaF
- Free Induction Decay (FID) detection of electronic transitions in an atomic beam!
- NOT detected by ion, e^- , or optical photon!
- 10^4 resolution elements in single shot, meaningful relative intensities (like NMR)
- 10^3 times better resolution than dye laser

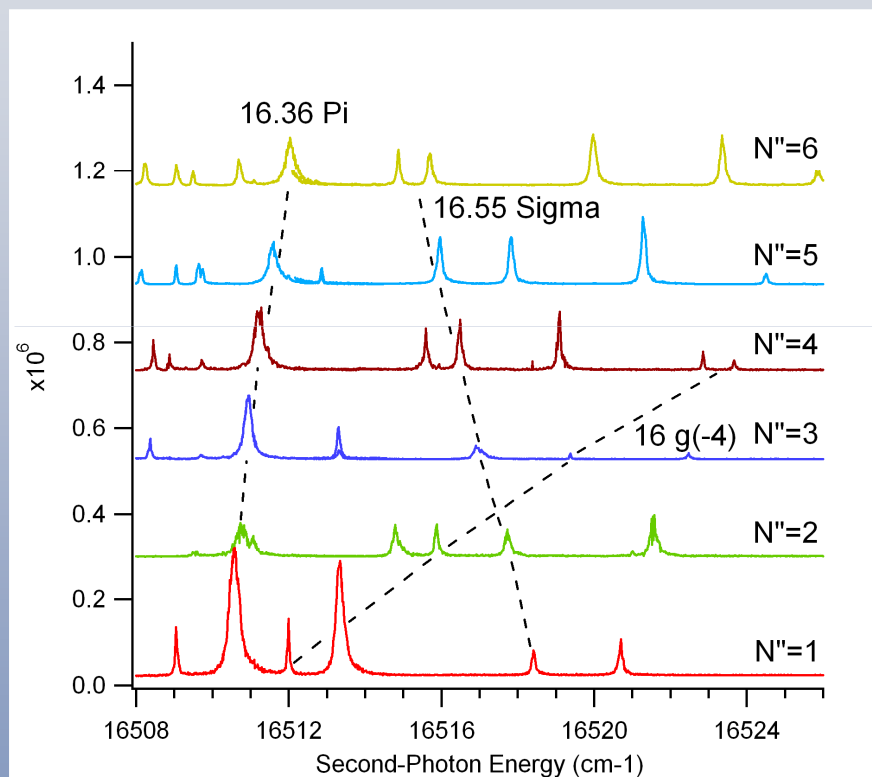
Experimental Methods

- Rydberg-Rydberg transitions in a supersonic molecular beam with a photoablation source of atoms/molecules
- 2 Color laser excitation to Rydberg states
- Resonance Enhanced Multiphoton Ionization (REMPI) *indirect* detection
 - 0.04 cm³ active volume
 - Must use very low laser pulse energy
- Chirped Pulse mmW: *direct* detection of Free Induction Decay
 - 100 cm³ active volume: 10⁸ Rydberg Atoms, 5 kDebye transition moments
 - Can use maximum laser pulse energy

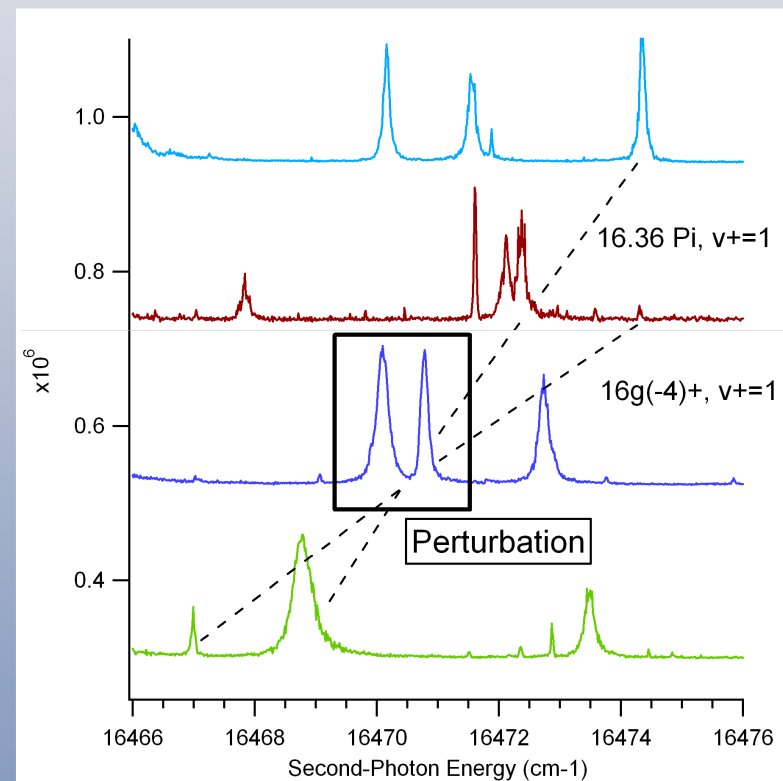
CaF Experimental Schemes



Linewidths, Perturbations, Stacked Plots

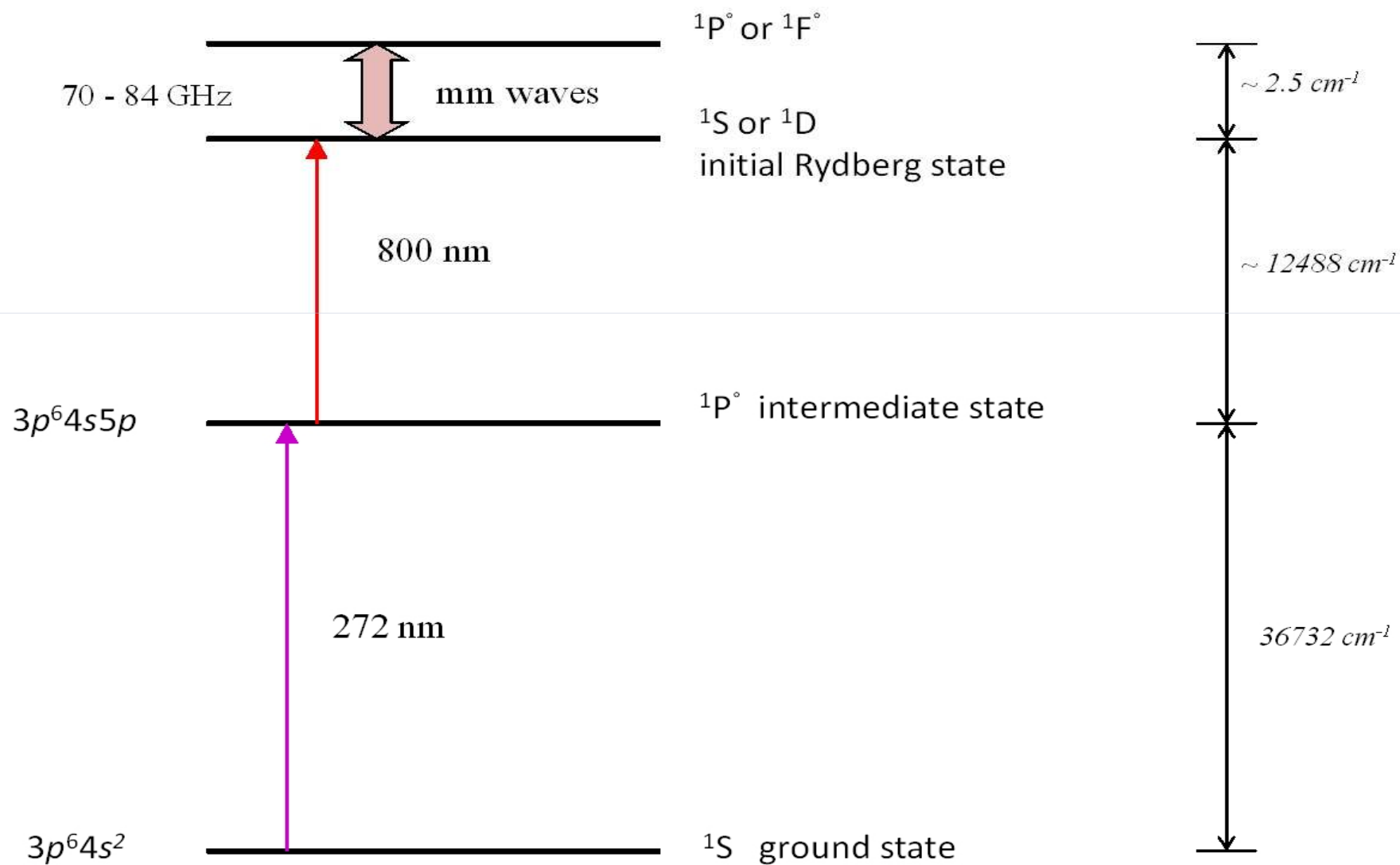


Some broad and some narrow lines

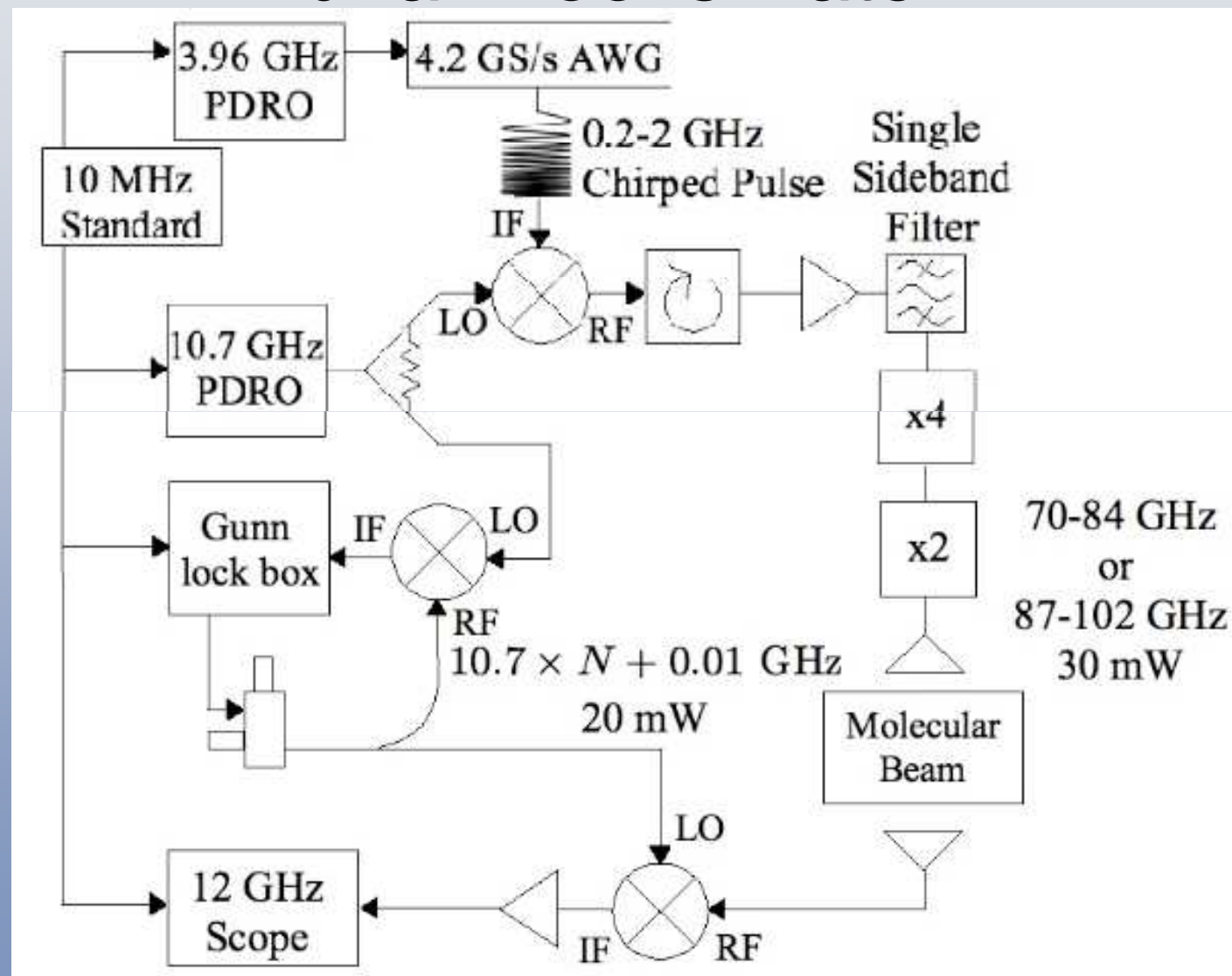


Intensity *and* linewidth sharing at a strong perturbation

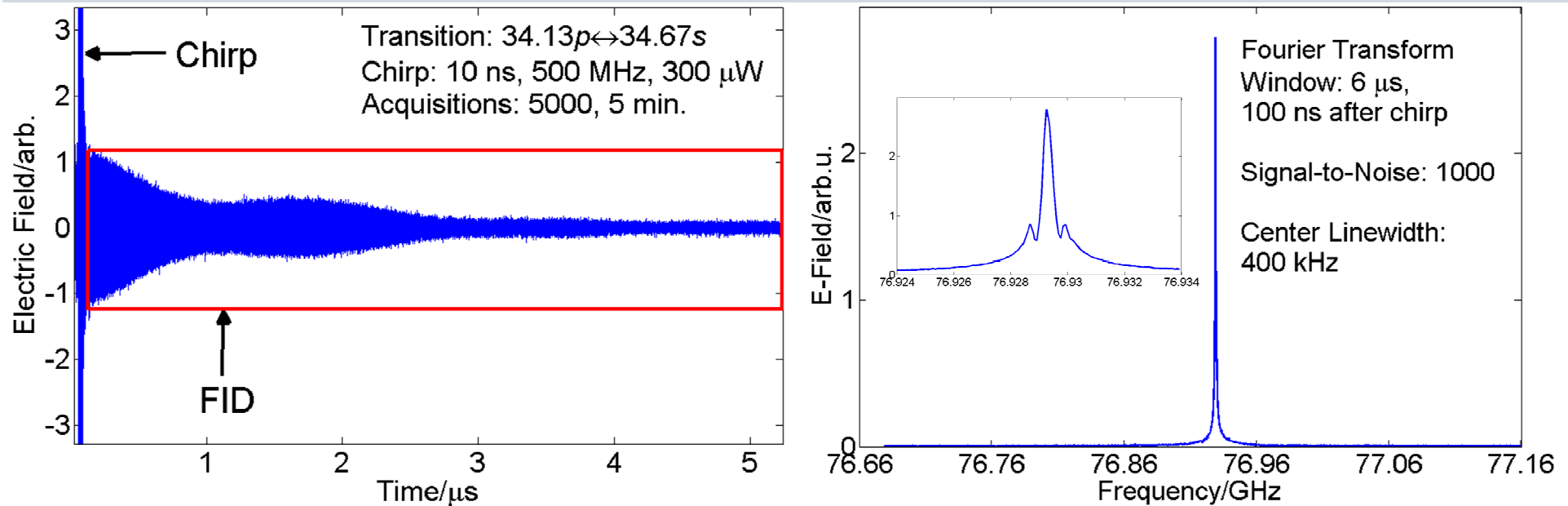
Level Diagram for **mm-Detected** Optical-Optical-mm Triple Resonance



Chirp Generation, FID Detection à la Brooks Pate



Our First Rydberg-Rydberg FID: Zeeman Splitting not Nulled



Rydberg Equation

$$E_{n\alpha\lambda} = -\mathcal{R}/(n - \mu_{\alpha\lambda})^2 = -\mathcal{R}/n^{*2}$$

n^* is the effective principal quantum number for the mixed- ℓ α, λ Rydberg series, \mathcal{R} is the Rydberg constant.

$\mu_{\alpha\lambda}$ is the eigen-quantum defect. Not a fudge factor! It is an eigenvalue of $\mu(R, E)$. $\pi\mu_{\alpha\lambda}$ is a phase shift.

$\mu(R, E)$ is the quantum defect matrix

Strongly R -dependent
Weakly E -dependent

Describes all spectra and all dynamics

We have experimentally determined all of the elements of the μ , $d\mu/dR$, and $d\mu/dE$ matrices.

Completeness of States Characterized: s~p~d~f Core-Penetrating Supercomplexes Plus f, g, and h Nonpenetrating States

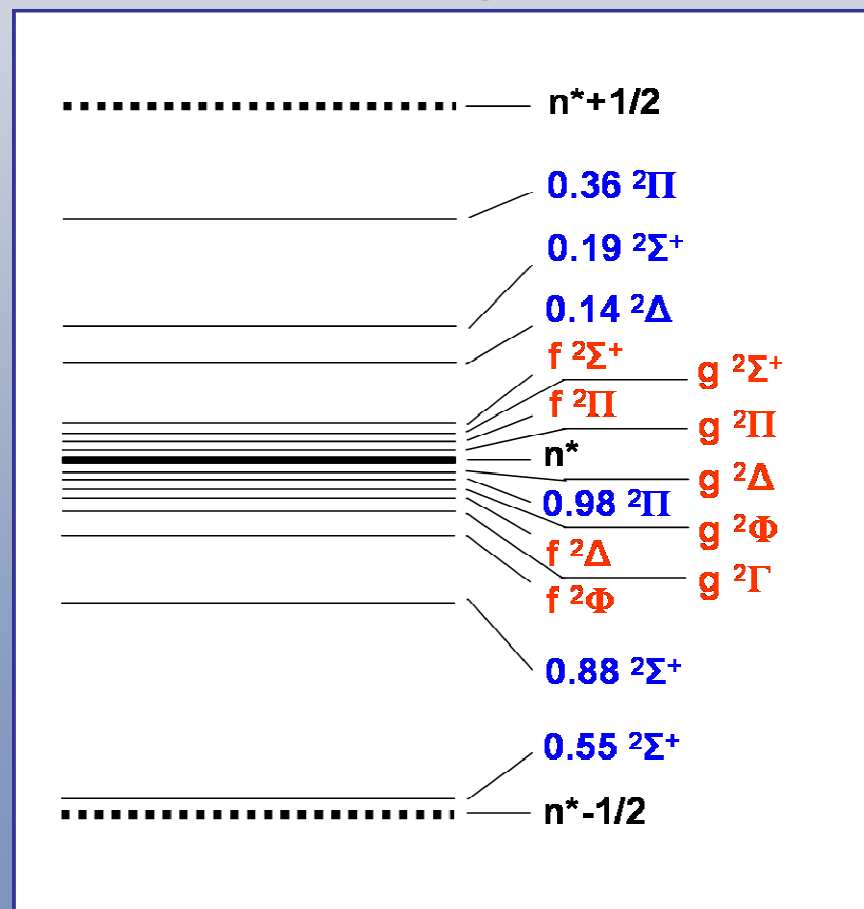
Eigenquantum Defects

	s	p	d	f
Σ	0.46	0.12	-0.18	-0.06
Π		-0.35	-0.04	-0.03
Δ			-0.12	0.03
Φ				0.1

Partial- ℓ Characters

	%s	%p	%d	%f
s Σ	85	14	1	1
p Σ	13	85	0	3
p Π		59	38	2
d Σ	3	0	56	41
d Π		40	50	10
d Δ			96	5
f Σ	0	2	42	56
f Π		1	11	88
f Δ			5	96
f Φ				100

Scaled Energy Level Pattern:
 n^* Template



Two Flavors of Rydberg States

- Core-Nonpenetrating: long range probe of ion-core multipole moments (μ, Q, O) and polarizability (α, γ)
 - Huge $|\Delta n^*| < 1$ transition moments, long lifetimes
 - Inside-out ligand field theory
 - Algebraic formulas: splittings $\rightarrow \mu, Q, O, \alpha, \gamma$ of ion
 - J. Chem. Phys. 128, 194301, (2008).
- Core-Penetrating: hard collisions of e^- with ion-core
 - Series terminus state encodes intra-core dynamics

Penetrating vs. Nonpenetrating Rydberg Orbitals

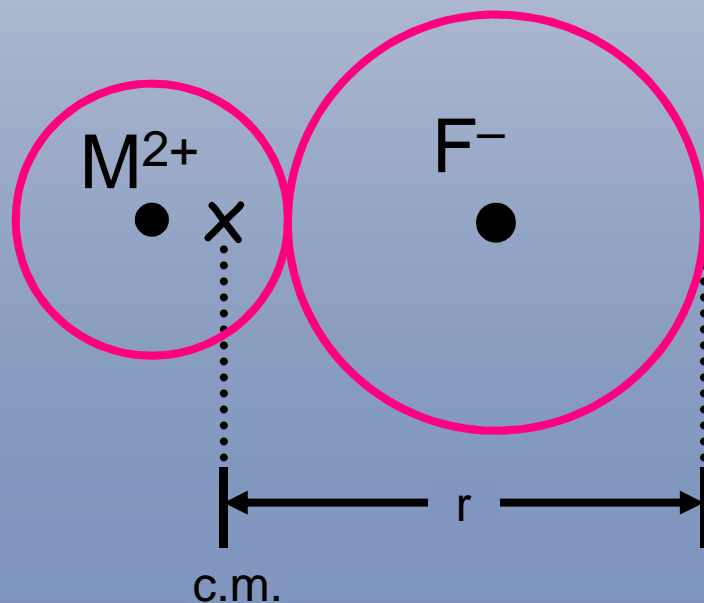
$$V_\ell(r) = -\frac{Z^{\text{eff}}(r)}{r} + \frac{\ell(\ell+1)}{2m_e r^2}$$

turning points

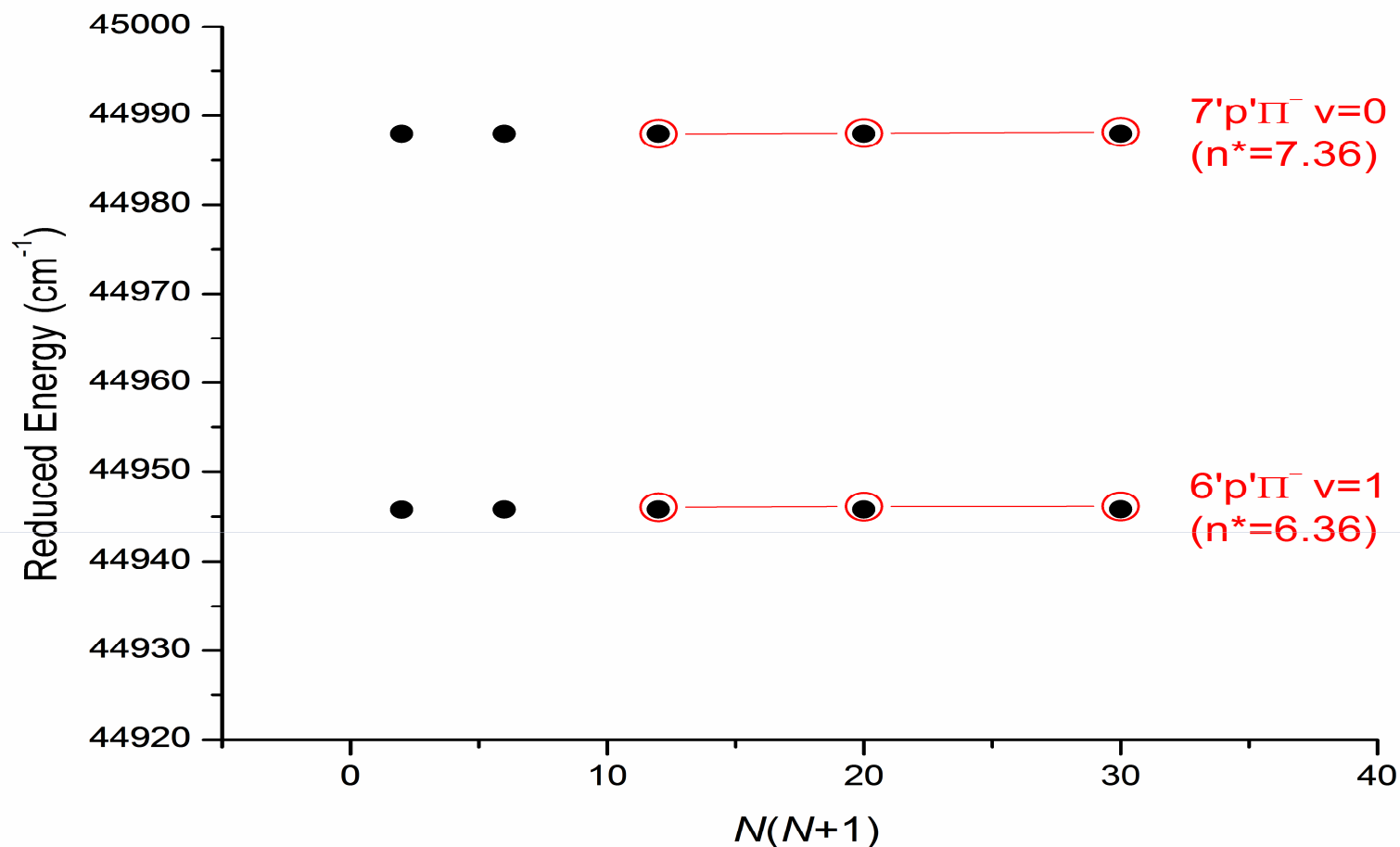
$$V_\ell(r_\pm) = E_{n\ell} = -\mathfrak{R}c/n^2$$

	$r_-/\text{\AA}$	$r_+/\text{\AA}$
2p	0.62	3.61
3d	2.06	7.51
4f	4.23	12.70
5g	7.32	19.14

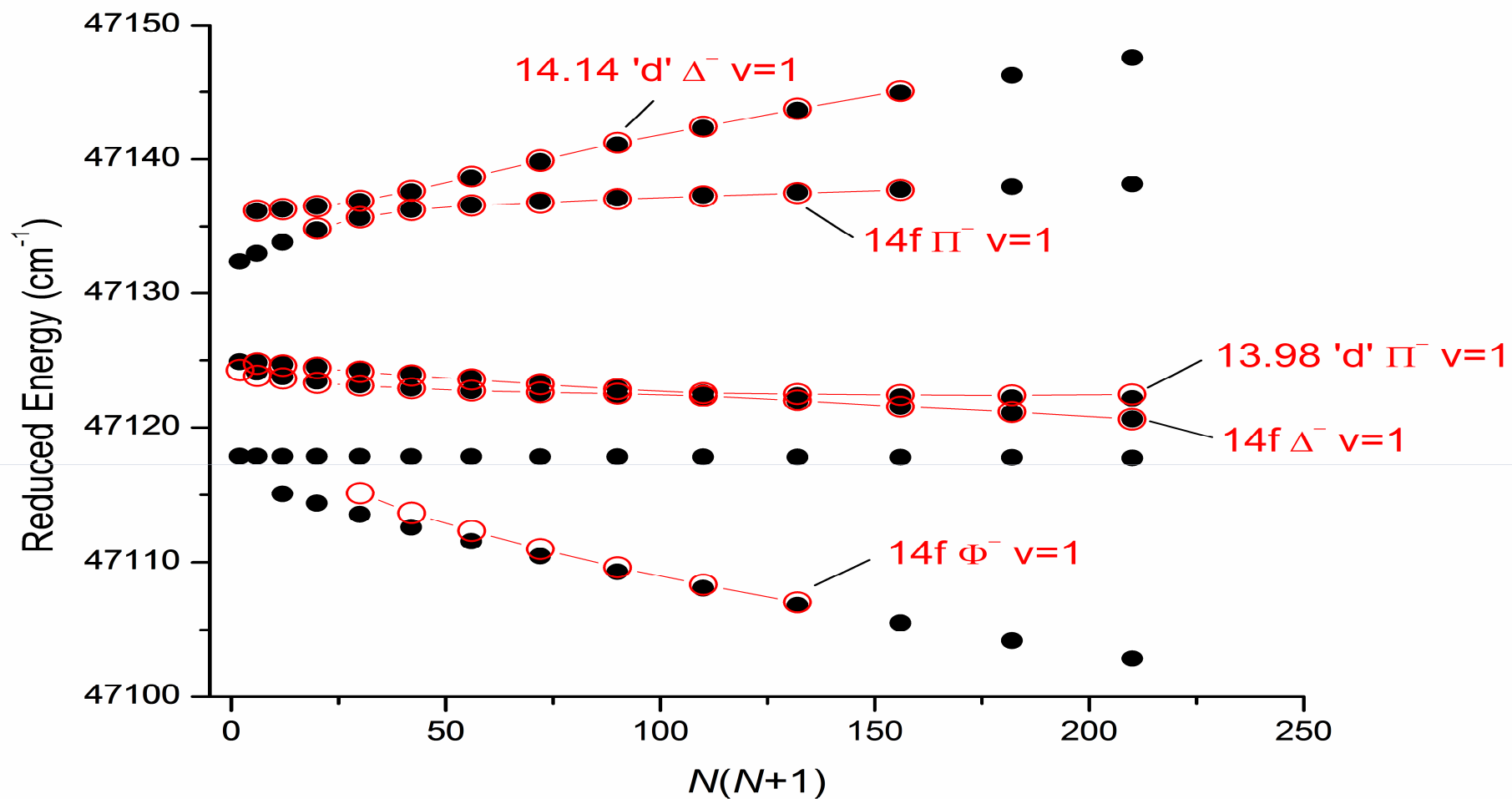
$$r_\pm = n^2 \left[1 \pm \left(1 - \frac{\ell(\ell+1)}{n^2} \right)^{1/2} \right] \text{ a.u.}$$



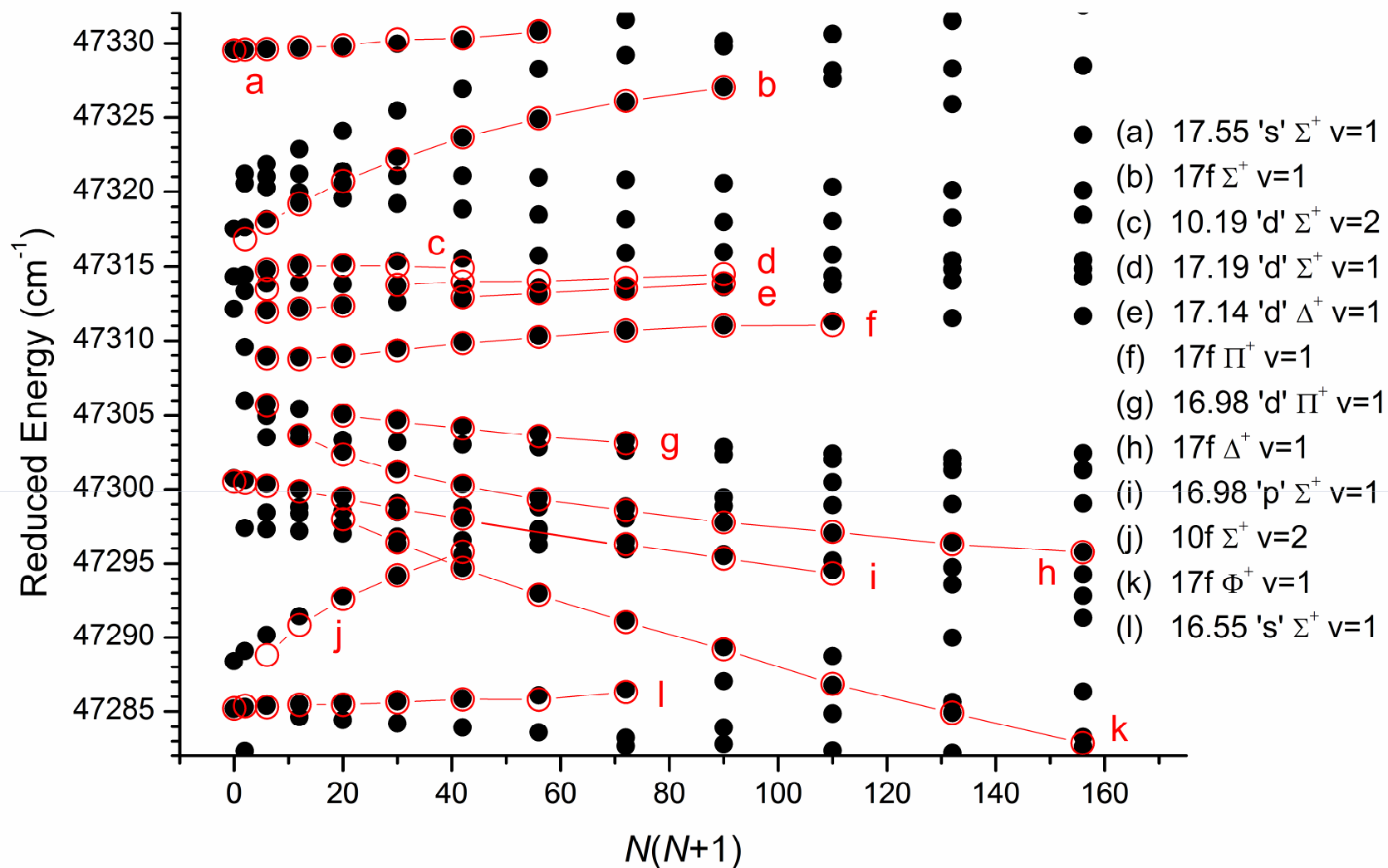
2.70 \AA for CaF^+
f should be nonpenetrating



Example of a strong $\Delta v^+=1$ perturbation. In the absence of the perturbation, the 7.36 'p' Π $v=0$ and 6.36 'p' Π $v=1$ levels are nearly degenerate. The **perturbation** causes a ~ 45 cm⁻¹ splitting of the levels and complete mixing of the wavefunctions. This same mechanism causes **vibrational autoionization**.



Quality of fit in the **14f complex**. A rotational perturbation between the 14f Π^- and the 14.14 'd' Δ^- **interloper** state gives rise to the avoided crossing at the top of the figure.



Quality of fit in the $n^* = 16.5 - 17.5$ region. Above $n^* \approx 16$, rotational interactions are strong and ubiquitous.

A Complete Model? (1)

$$\mu^{(N,\lambda,parity)}(R,E) = \mu(R_e^+, E=0) + \frac{\partial\mu}{\partial R}(R-R_e^+) + \frac{\partial\mu}{\partial E} E$$

ALL ENERGY LEVEL SPLITTINGS $E_{n^{*+\delta/2}} - E_{n^{*-\delta/2}} = \frac{2c\Re\delta}{n^{*3}}$

ALL OFF-DIAGONAL MATRIX ELEMENTS OF EVERYTHING

$$\langle n^* | \mathbf{A} | n^{*'} \rangle = A_0 (n^* n^{*'})^{-3/2}$$

n^* -scaling of ω_{e,n^*} , B_{e,n^*} , etc.

ALL SPECTRA

ALL DYNAMICS

Once $\mu(R_e^+)$, $\left. \frac{\partial\mu}{\partial R} \right|_{R_e^+}$, and $\left. \frac{\partial\mu}{\partial E} \right|_{R_e^+}$ are determined,

the picture is complete.

A Complete Model? (2)

$$\mu^{(N,\lambda,parity)}(R, E) = \mu(R_e^+, E=0) + \frac{\partial \mu}{\partial R}(R - R_e^+) + \frac{\partial \mu}{\partial E} E$$

ALL ENERGY LEVEL SPLITTINGS $E_{n^{*+\delta/2}} - E_{n^{*-\delta/2}} = \frac{2c\mathfrak{R}\delta}{n^{*3}}$

ALL OFF-DIAGONAL MATRIX ELEMENTS OF EVERYTHING

$$\langle n^* | \mathbf{A} | n^{*'} \rangle = A_0 (n^* n^{*'})^{-3/2}$$

n^* -scaling of ω_{e,n^*} , B_{e,n^*} , etc.

ALL SPECTRA

ALL DYNAMICS

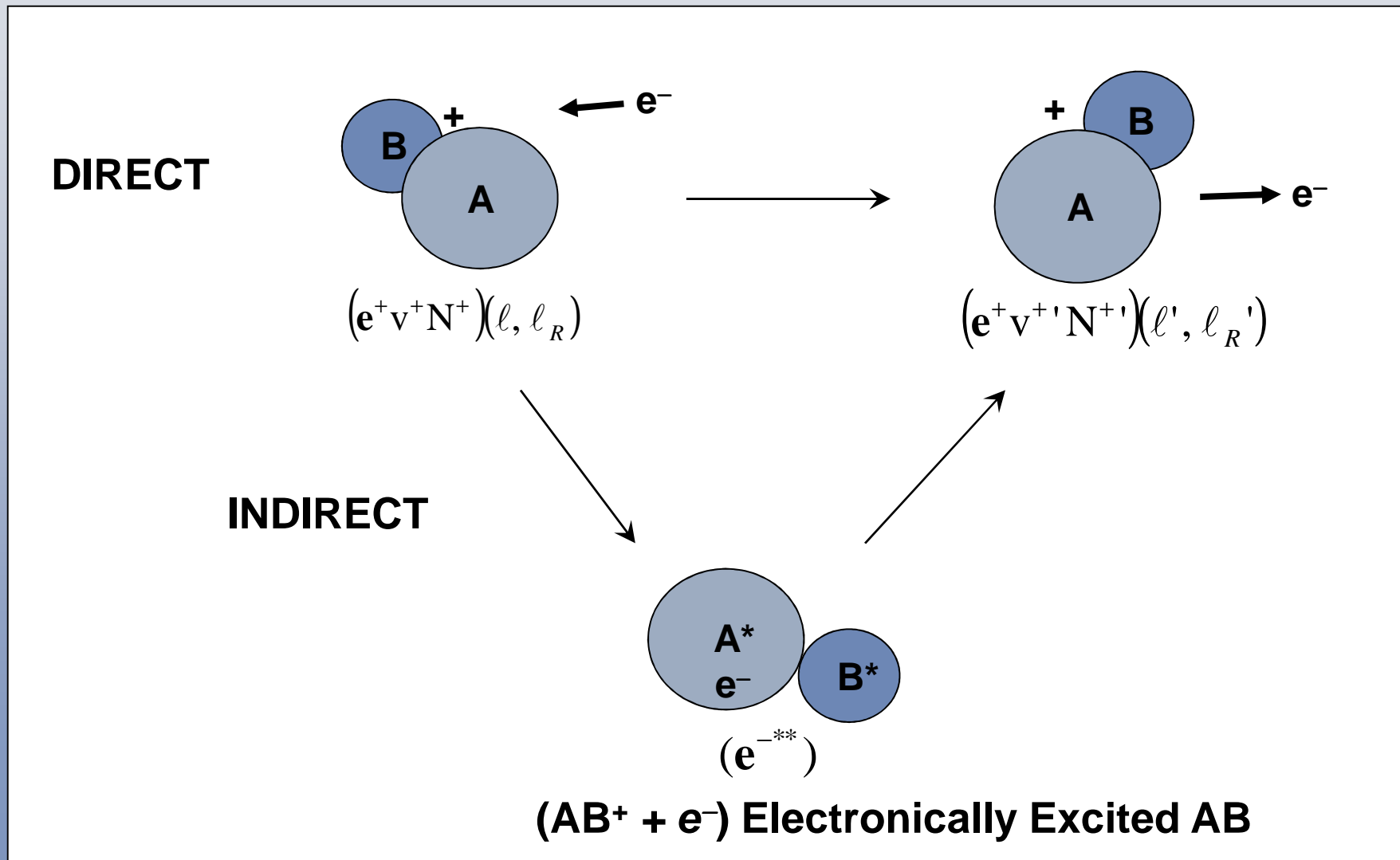
Once $\mu(R_e^+)$, $\left. \frac{\partial \mu}{\partial R} \right|_{R_e^+}$, and $\left. \frac{\partial \mu}{\partial E} \right|_{R_e^+}$ are determined,

the picture is complete.

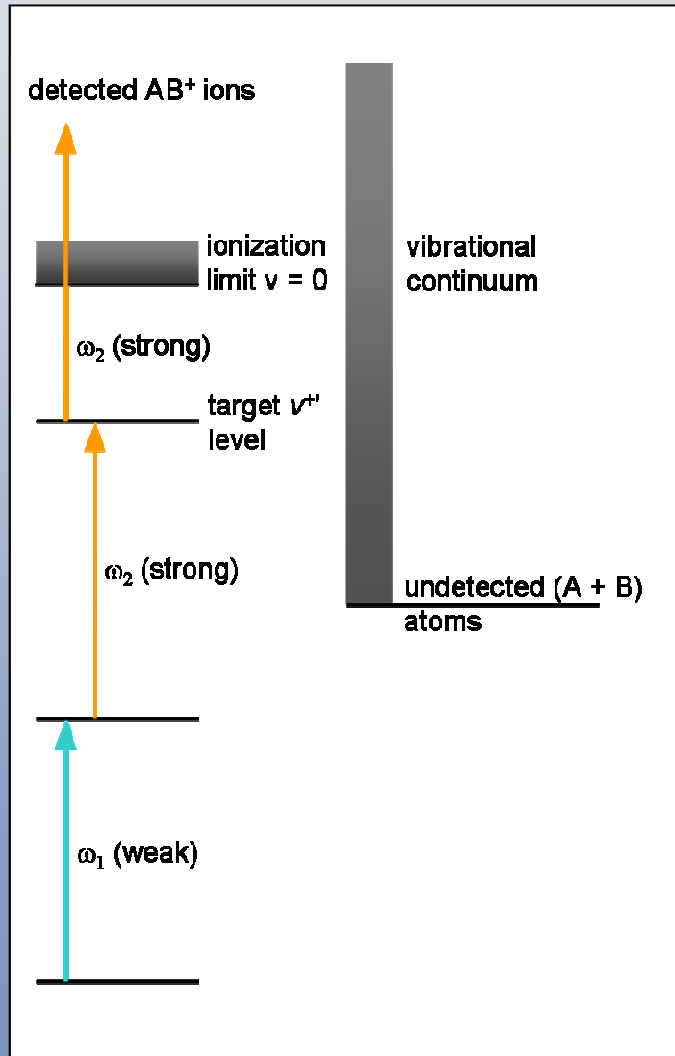
Or is it?

Presence of indirect processes!

Indirect Processes



Signatures of Indirect Processes



- $\Delta v^+ = 0$ Franck-Condon propensity rule grossly violated
 - (A+B) continuum \leftarrow intermediate
 - $AB^+ + e^- \leftarrow$ (A+B) continuum
-] electronic transitions violate 1- e^- selection rule

Yet asymmetric (Fano) lineshapes

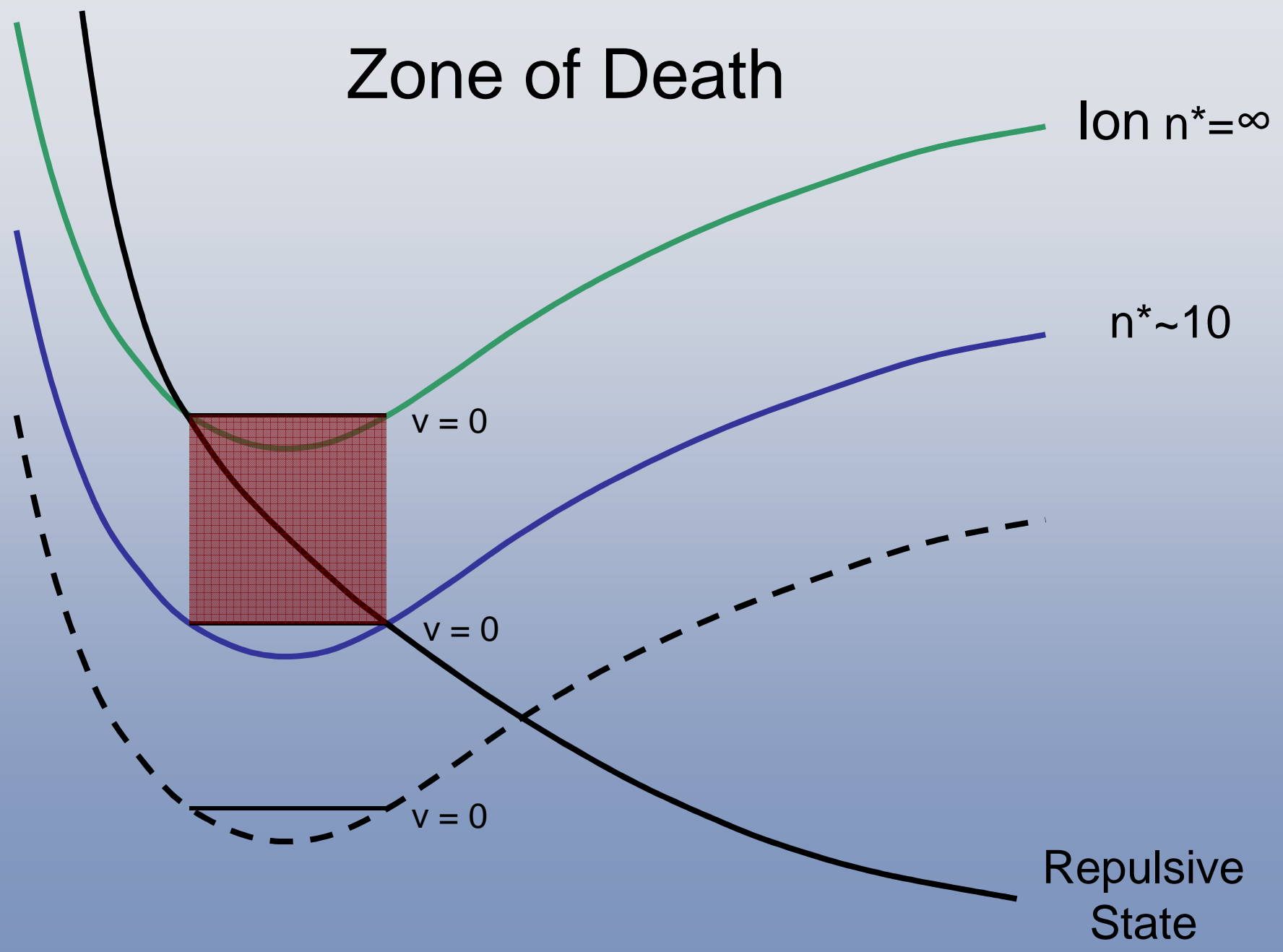
- Quasi-continuous 2-photon non-resonant background overwhelms 2-step resonant sharp lines
- $(AB^+ v^+, N^+) + (e^- \ell, \ell_R)$ photofragments produced in states not consistent with $\mu(R)$

Every experimental observation seems to demand a special explanation

No big picture

But in CaF, all indirect processes are due to **only one repulsive curve**

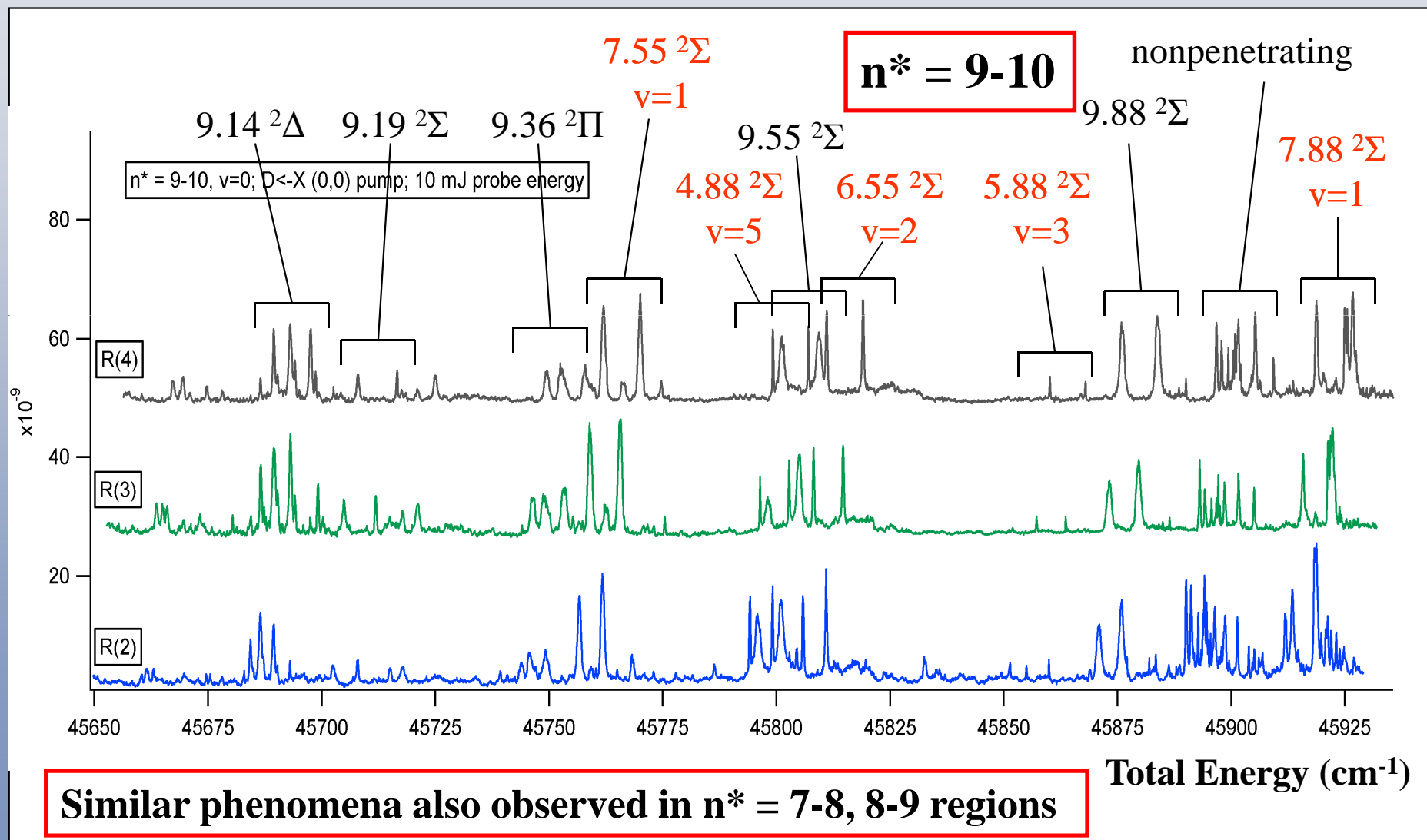
Zone of Death



Zone of Death

- Short Lifetimes
 - Predissociation, Autoionization
 - Too short for FID detection
 - Too short for exotic applications
- Indirect Processes
 - One repulsive state shatters all propensity rules
- Rydberg Electron \leftrightarrow Ion-Core energy exchange:
scales as n^{*-3} , $\sim \ell^{-10}$ (for $\ell > 3$: Gallagher p. 410)
- Jump over the zone of death? High- ℓ states!
 - NMR-esque pulse gymnastics

Spectra Grossly Violate $\Delta v=0$ Franck-Condon Propensity Rule



Observed Wrong- ν Transitions Are Exclusively Σ

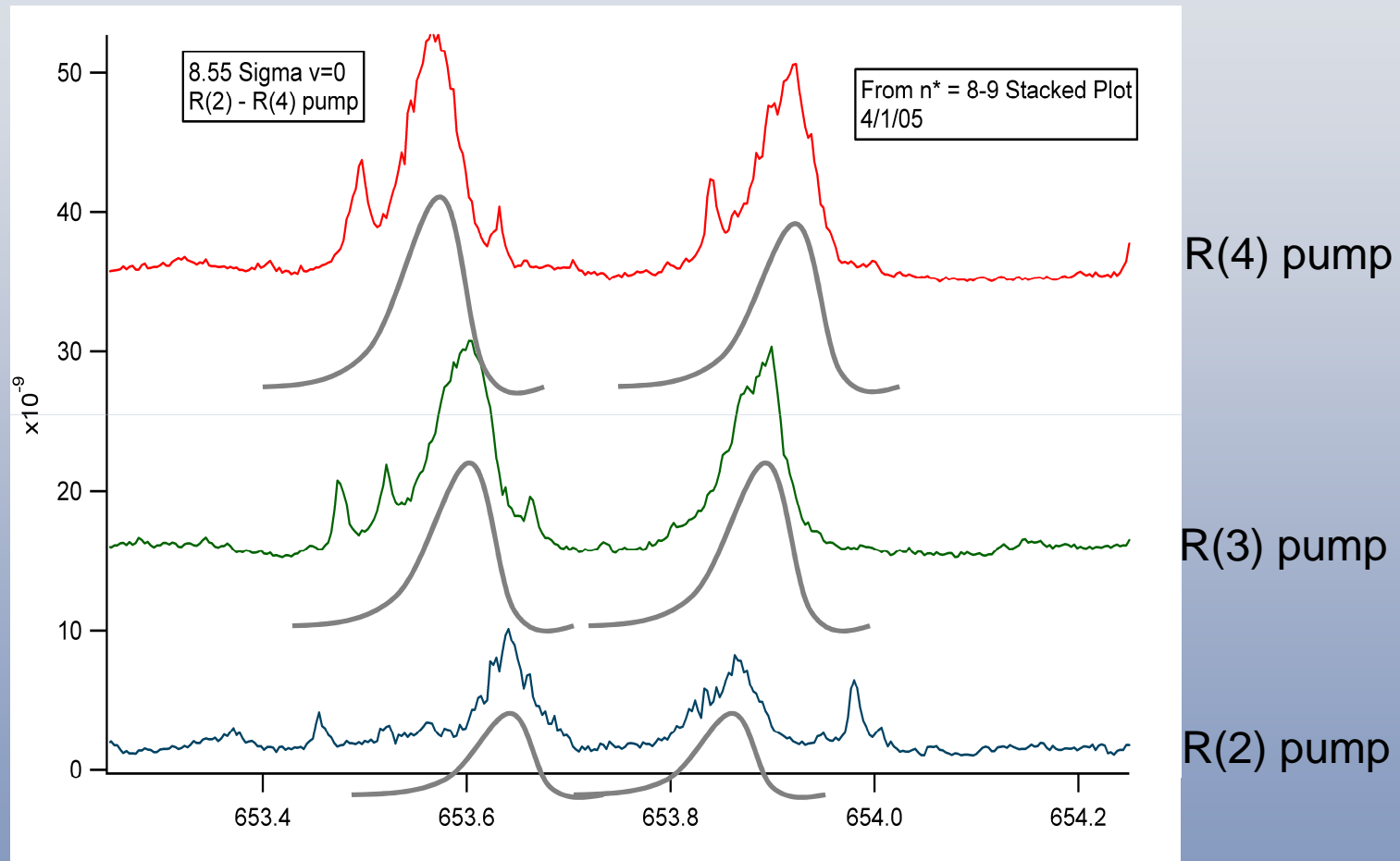
ν	Series	Symmetry	Observed?
0	8.19	Σ	✓
0	8.36	Π	✓
0	8.55	Σ	✓
0	8.88	Σ	✓
0	8.98	Π	✓
0	9.14	Δ	✓
0	9.19	Σ	✓
0	9.36	Π	✓
0	9.55	Σ	✓
0	9.88	Σ	✓
1	6.88	Σ	✓
1	6.98	Π	✓
1	7.14	Δ	x
1	7.19	Σ	✓
1	7.36	Π	✓
1	7.55	Σ	✓
1	7.88	Σ	✓

ν	Series	Symmetry	Observed?
2	6.14	Δ	x
2	6.19	Σ	✓
2	6.36	Π	x
2	6.55	Σ	✓
3	5.55	Σ	✓
3	5.88	Σ	✓
4	5.14	Δ	x
4	5.19	Σ	x
4	5.36	Π	x
5	4.88	Σ	✓

Electronic transition moment **large**

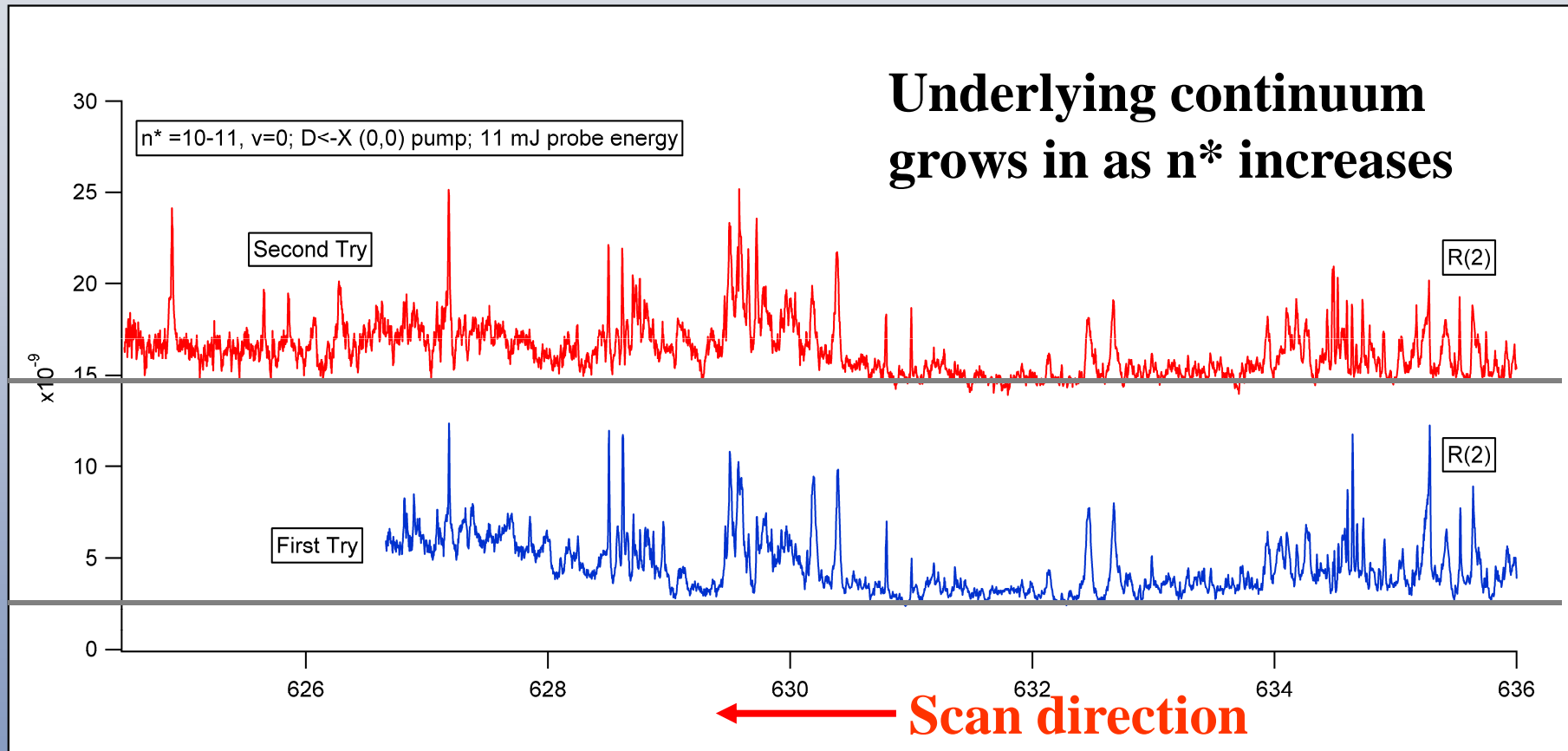
All $\nu > 1$ states that appear in spectrum are ${}^2\Sigma^+$ states

Fano Lineshapes



Asymmetric Lineshapes: interference between transition amplitudes
(But how? Transitions into repulsive state are forbidden.)

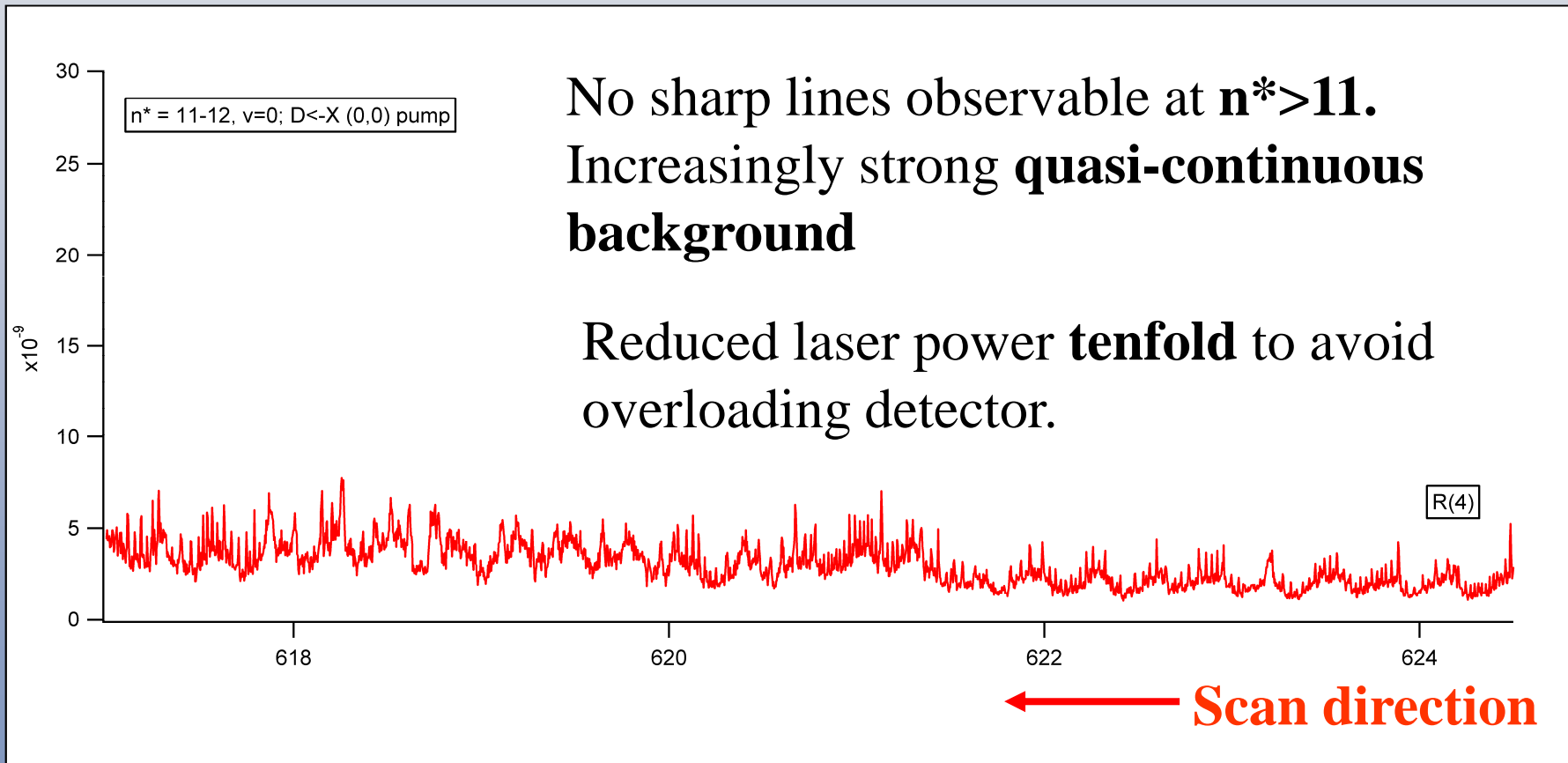
Spectra at Higher Energy: $n^*=10-11$



Not a decreasing intensity artifact
of Ca rod ablation

Scans performed from
low to **high** frequency

Spectra at Higher Energy: $n^*=11-12$



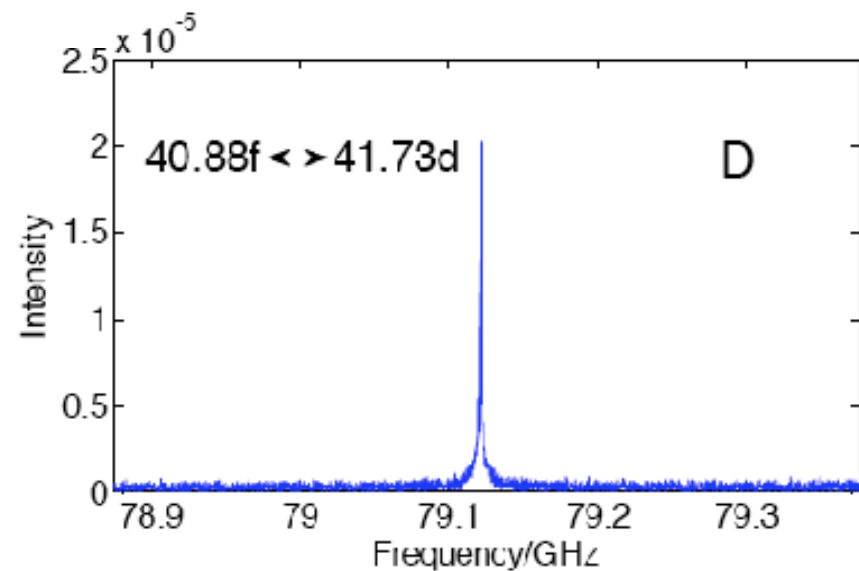
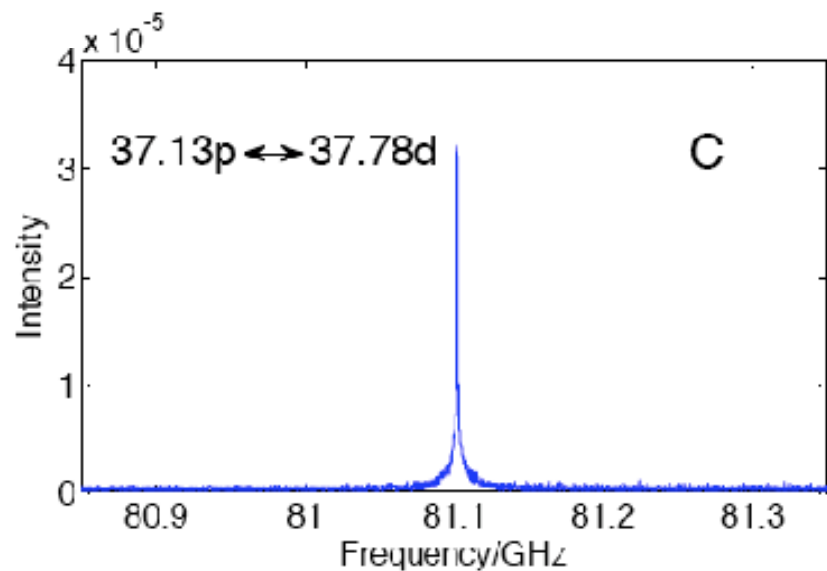
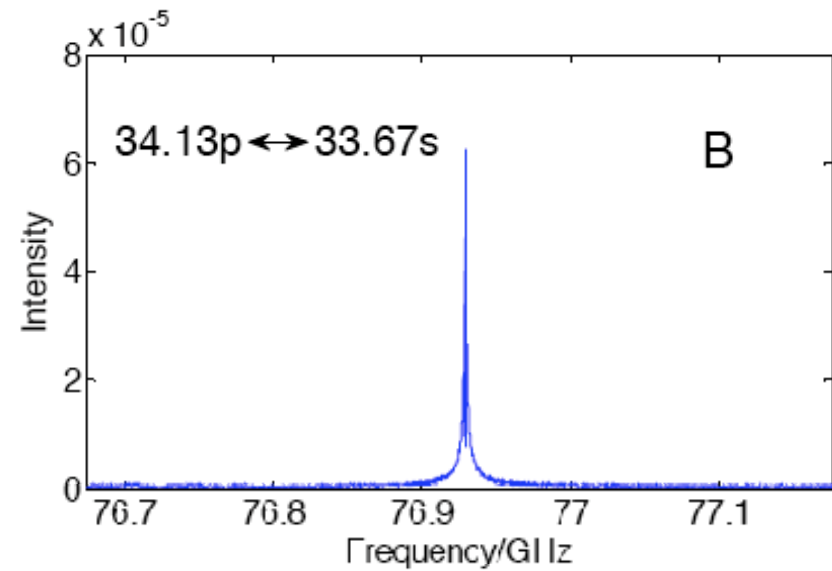
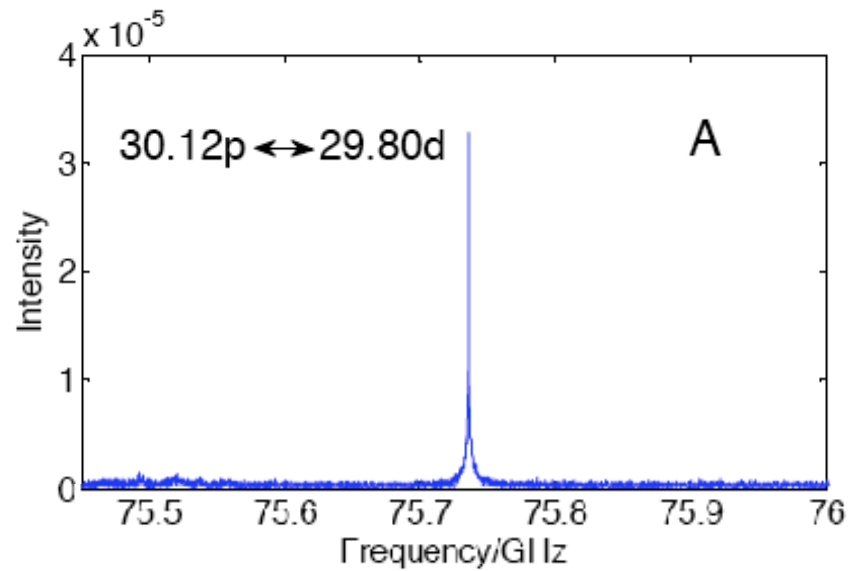
All Surprising Observations Are Explained by “Indirect” Process

- Mediated by $\text{Ca}(4s^2)\text{F}(2p\sigma^{-1})$ Vibrational Continuum
- Wrong Δv transitions
- Fano Lineshapes
 - $\text{Ca}^{2+}\text{F}^- e^-_{\text{Ry}} \rightarrow \text{Ca}(4s^2) + \text{F}(2p\sigma^{-1})$ dissociation continuum transition is forbidden ($2 e^-$)
 - $\text{Ca}(4s^2)\text{F}(2p\sigma^{-1}) \rightarrow \text{Ca}^{2+}\text{F}^- + e^-$ ionization continuum transition is forbidden ($2 e^-$)
- Quasi-Continuum

Rydberg-Rydberg Spectra of Ca Atom

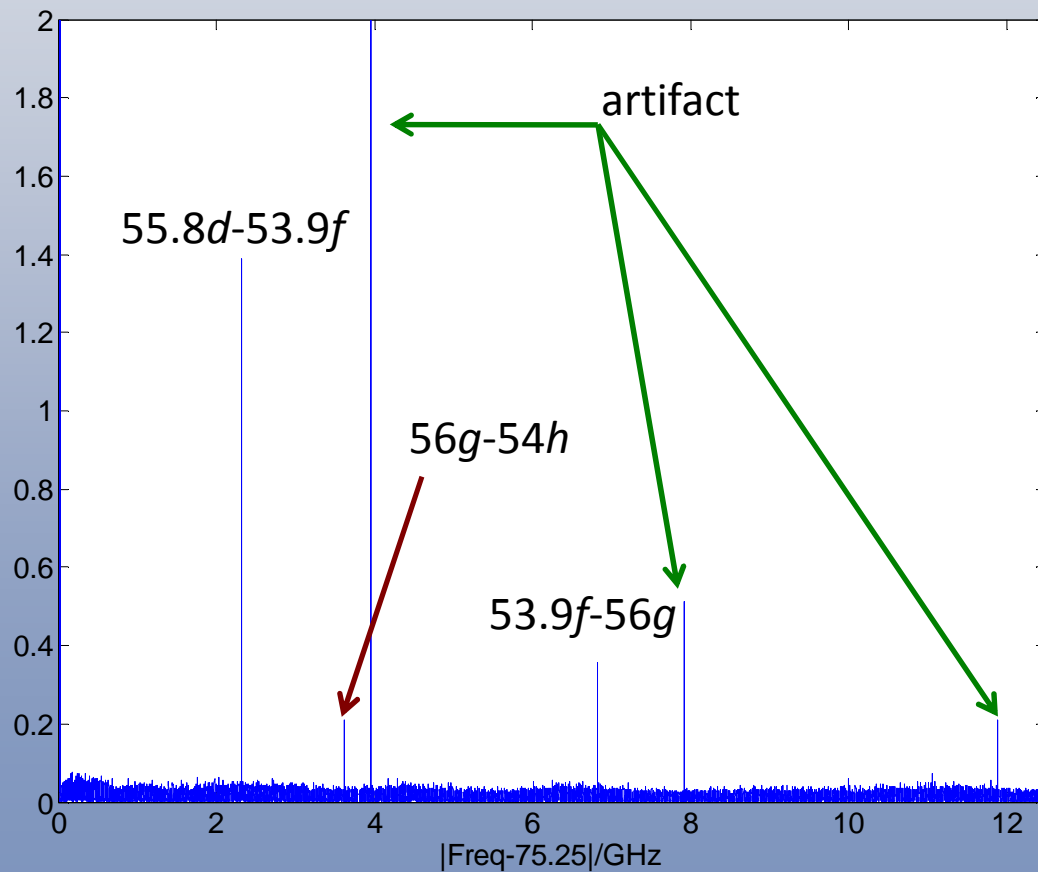
- Optical-Optical-mm Triple Resonance
- **FID Detected** (FID duration $>1 \mu\text{s}$)
 - Chirp duration as short as 10 ns
- Crucial apparatus modification: $0.04 \rightarrow 100 \text{ cm}^3$
- 10 GHz search at 1 MHz resolution
- Extend to molecules? Pure electronic spectra?
- Nonpenetrating molecular states
 - $\Delta v^+ = 0, \Delta J^+ = 0$ ion-core transition selection rules
 - Lifetimes as long as 1 ms
- Must turn off predissociation and autoionization
 - Exploit n^{-3}, ℓ^{-10} scaling

FID-Detected Ca Atom Rydberg-Rydberg Electronic Transitions



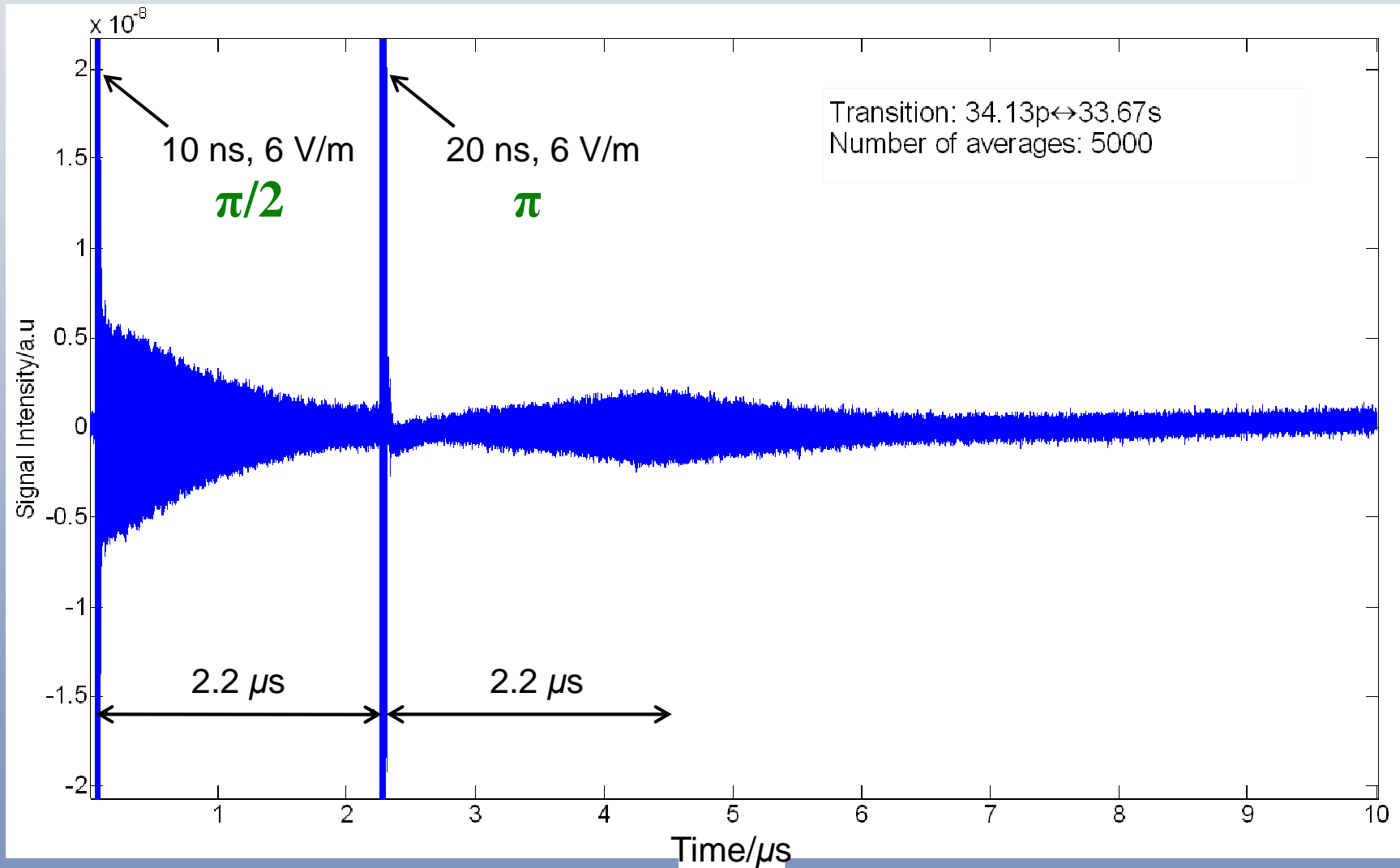
Climbing a ladder

55.8*d* $\xrightarrow{73\text{GHz}}$ 53.9*f* $\xrightarrow{82\text{GHz}}$ 56*g* $\xrightarrow{79\text{GHz}}$ 54*h* $\xrightarrow{80\text{GHz}}$ 56*i*

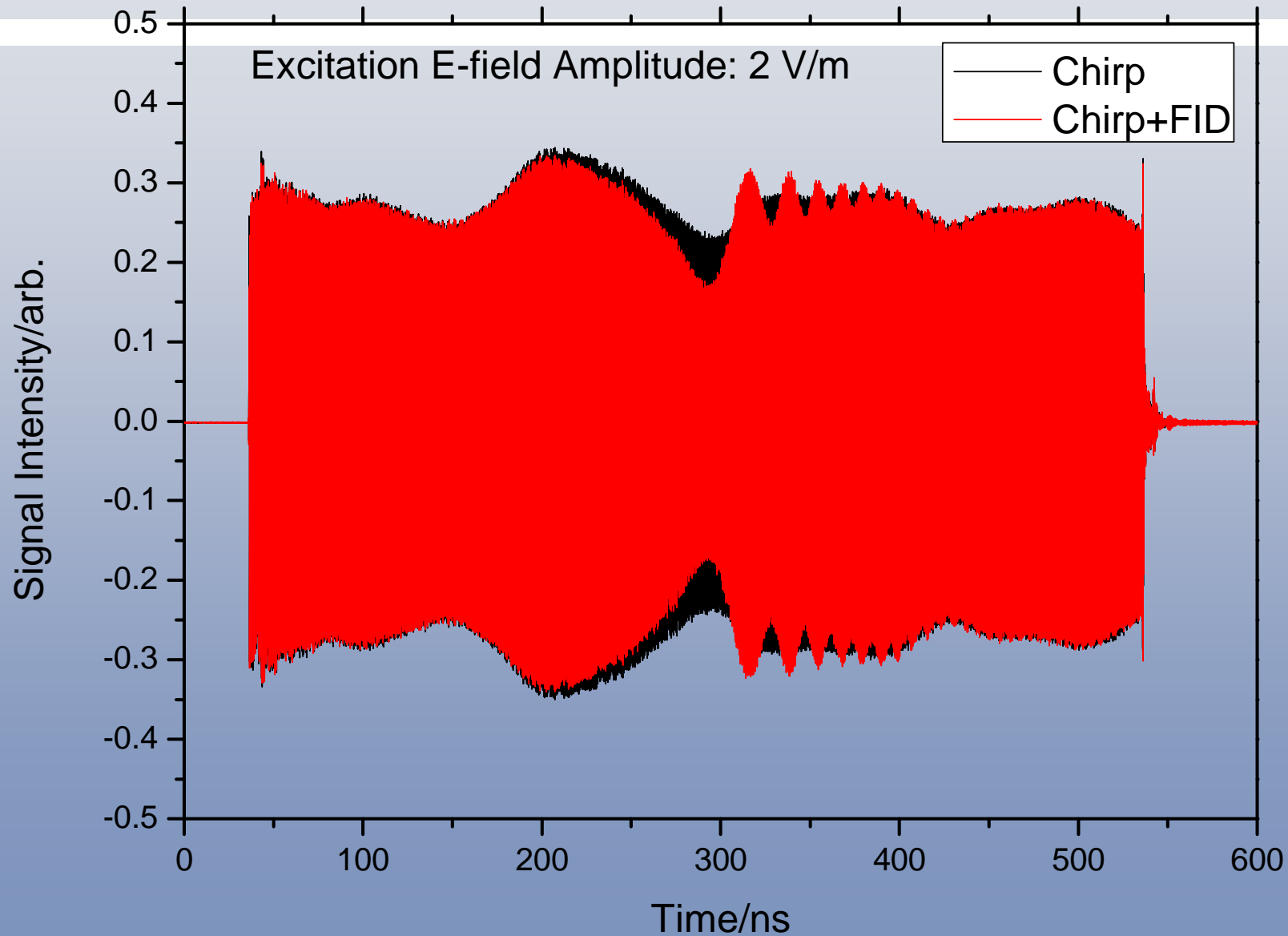


5,000 averages

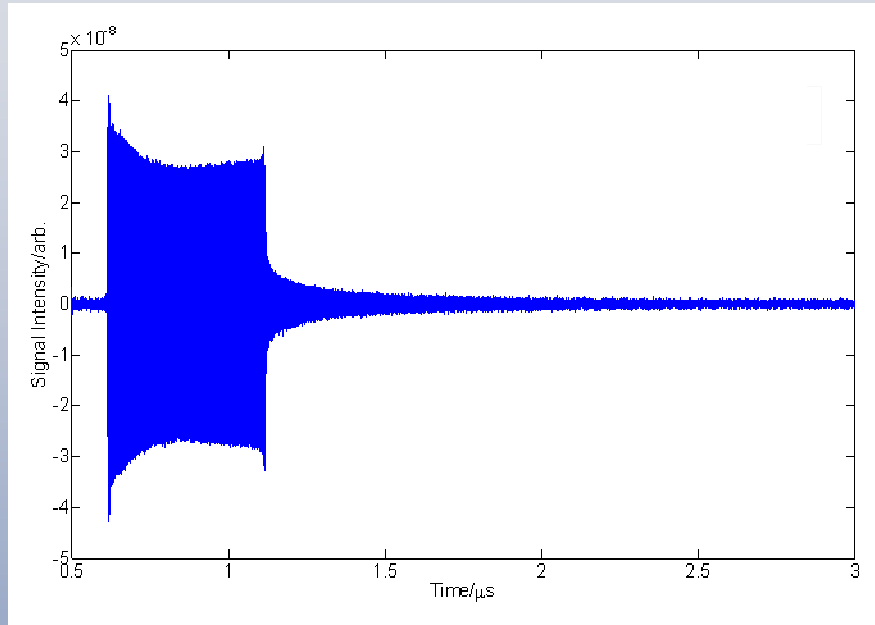
Millimeter-Wave Photon Echo



FID During a Chirp

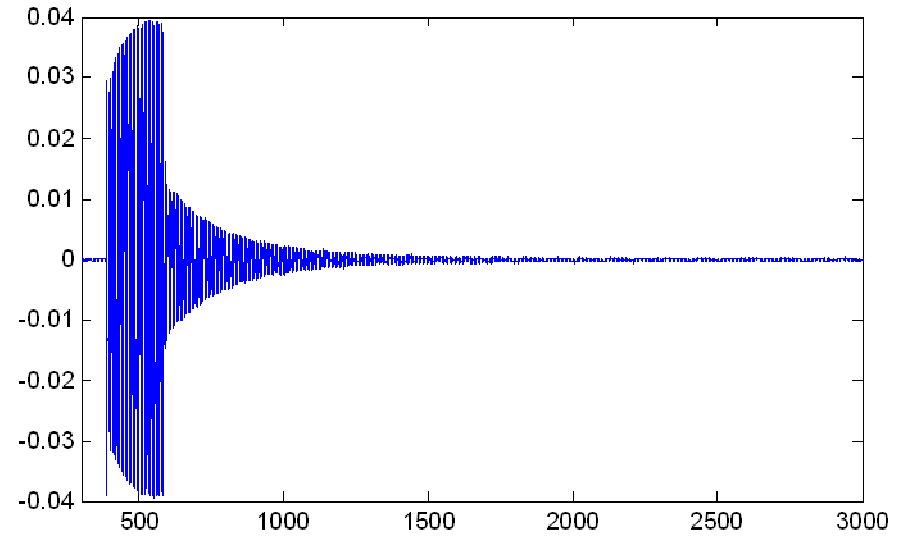


Which way is up?



Time/ μs

34.13p
33.67s



Time/ns

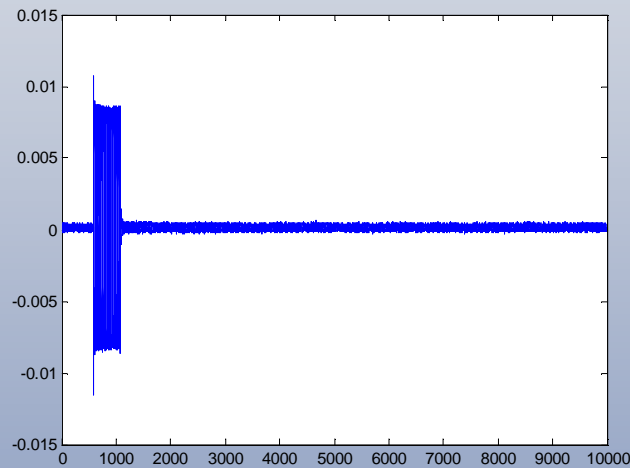
41.73d
40.88f



Calcium Atoms

Fitted Phase Difference: FID-mmW Pulse

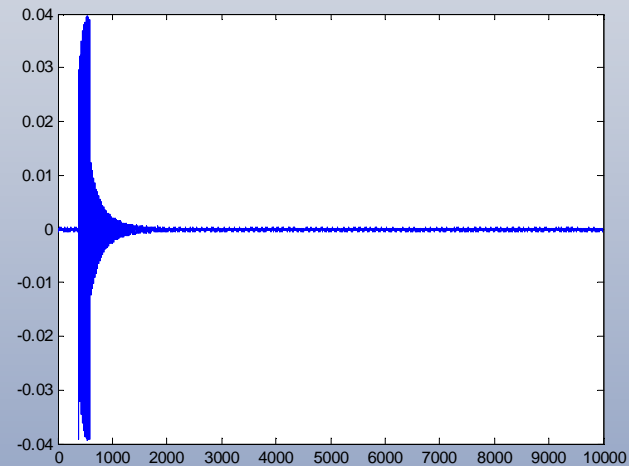
$34.13p - 33.67s$



$1.08(2) \pi$

Single frequency excitations

$41.73f - 40.88d$

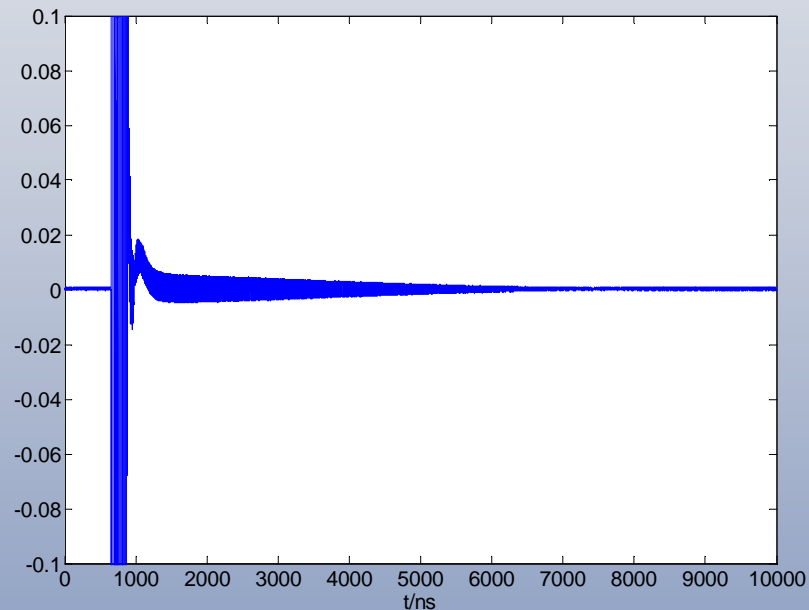


$0.04(1) \pi$

Uncertainties in () are the 95% confidence intervals

SO₂: $\pi/100$ Polarizing Pulse Chirp-FID Phase Difference

$$6_{06} - 5_{15}$$



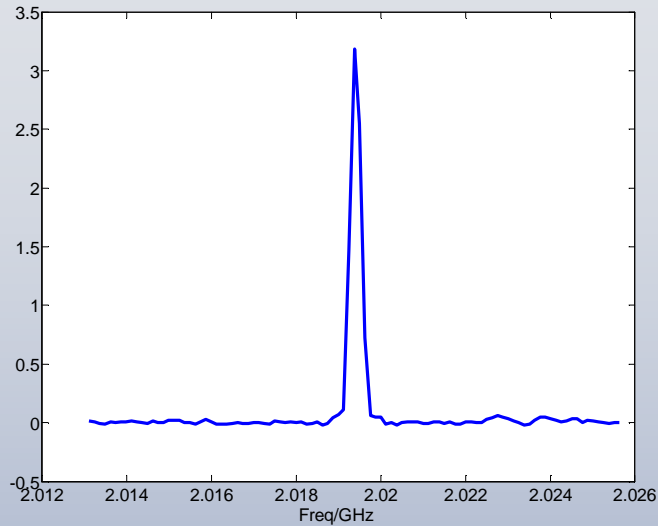
$$1.01(2) \pi$$

Oscilloscope truncated-Chirp, fitted to only ~1% of the chirp amplitude
chirp duration 500 ns
chirp bandwidth 5 GHz

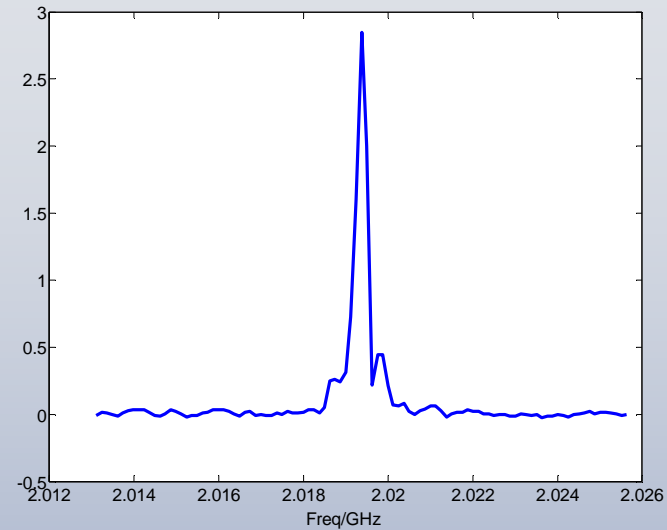
Uncertainty in () is 95% confidence interval

“Optical” Nutation: A Small Step from Superradiance

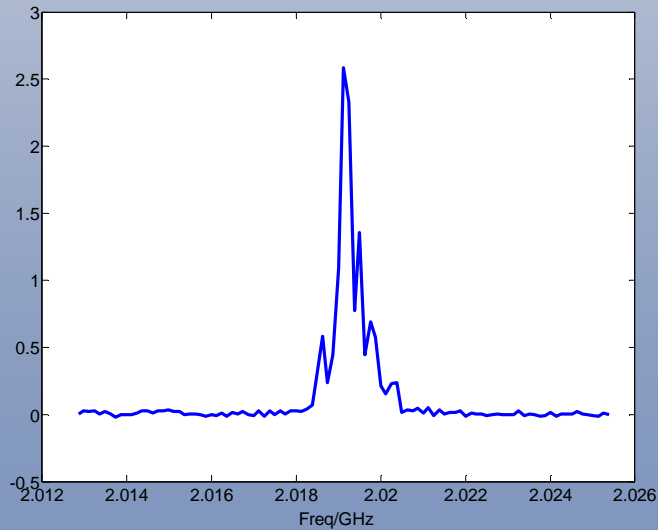
$N < 1 \times 10^5/\text{cm}^3$, $\sim \pi/2$ ex_pulse



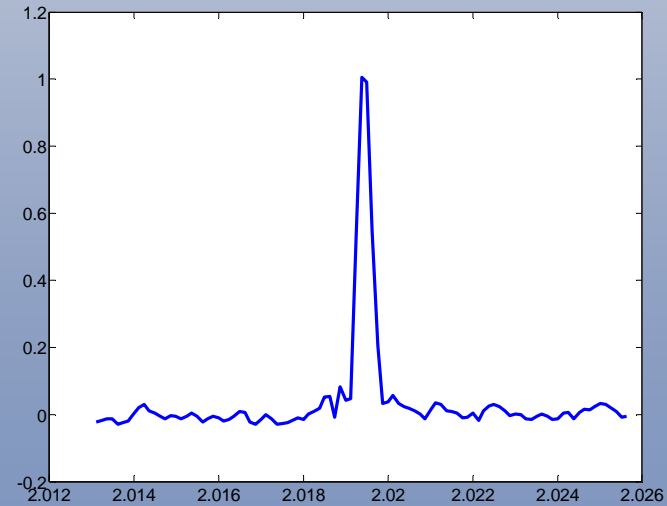
$N \sim 1 \times 10^5/\text{cm}^3$, $\sim \pi/2$ ex_pulse



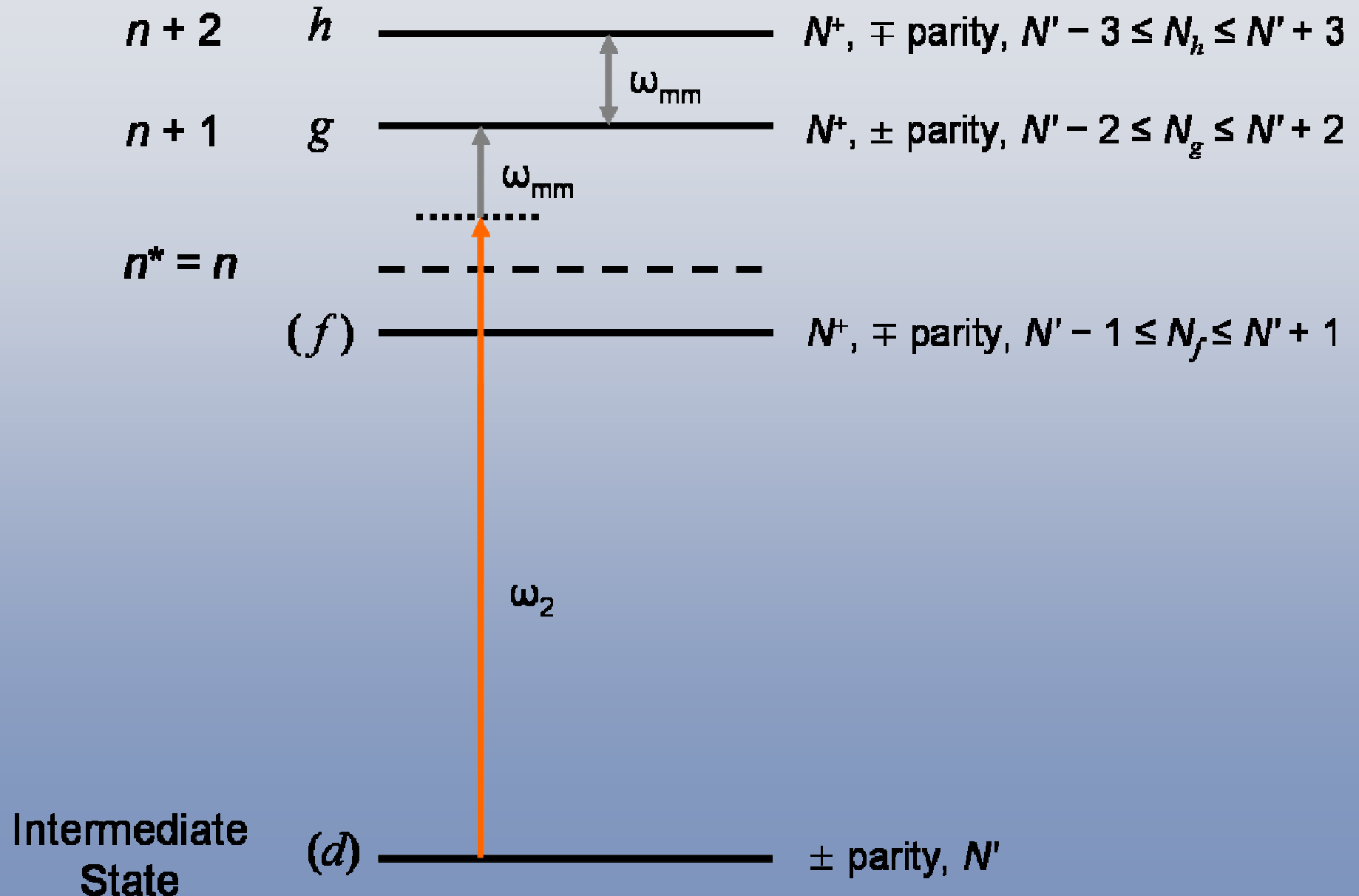
$N \sim 3 \times 10^5/\text{cm}^3$, $\sim \pi/2$ ex_pulse



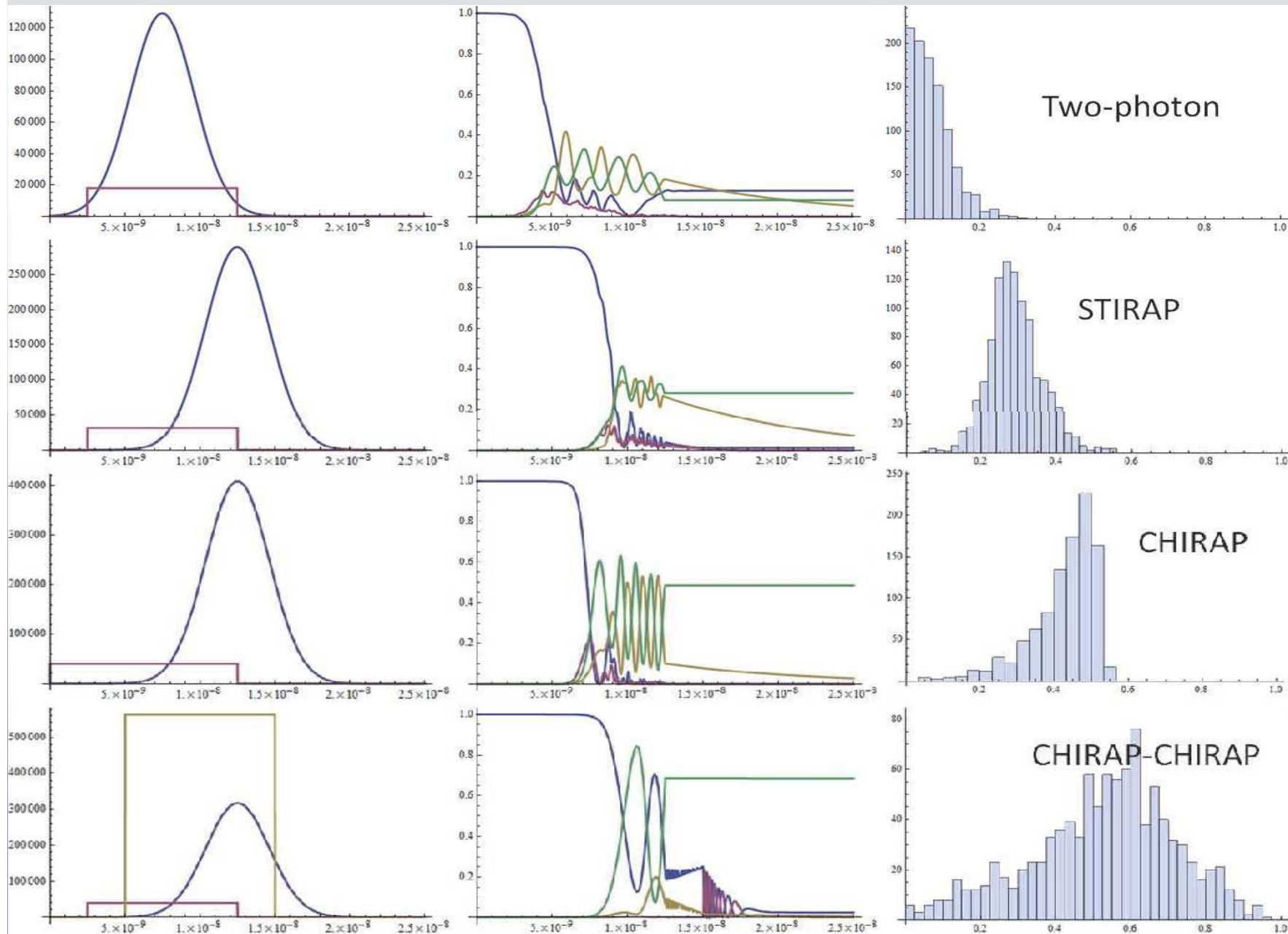
$N \sim 3 \times 10^5/\text{cm}^3$, $\sim \pi$ ex_pulse



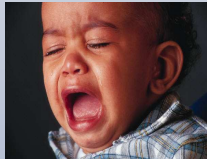
How to Jump Over the Zone of Death



Jumping Over the Zone of Death



Conclusions

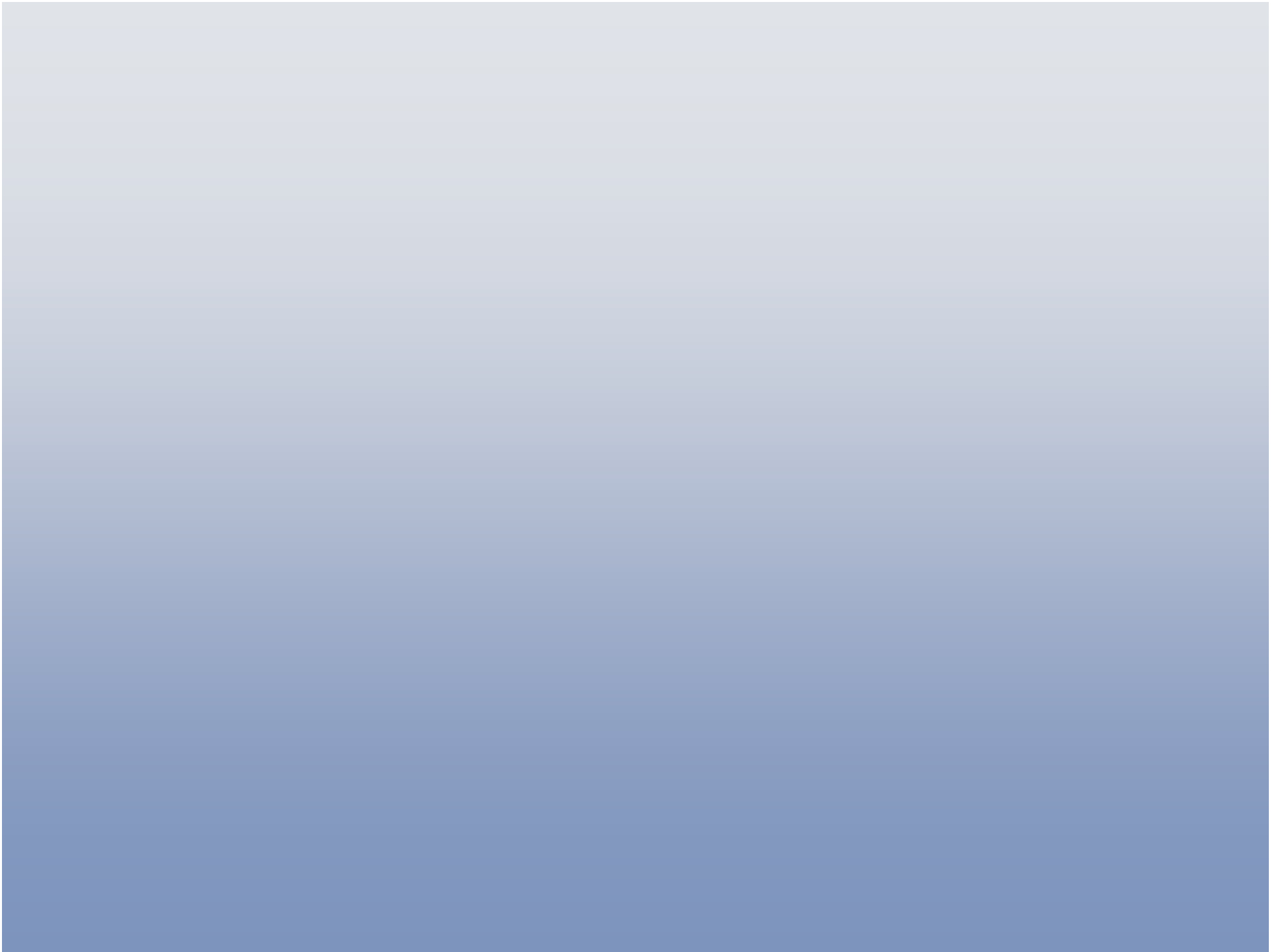
- CaF: complete experimental determination of quantum defect matrix
 - All spectra, all dynamics!
- Tedious detective work:  or  ?
- Need higher resolution, meaningful intensities, and escape from fast nonradiative decay
- FID-detected Rydberg-Rydberg spectra!
 - $>10^3$ Debye transition moment at $n^* \approx 20$
 - pure electronic Rydberg-Rydberg spectra

Who Did This?

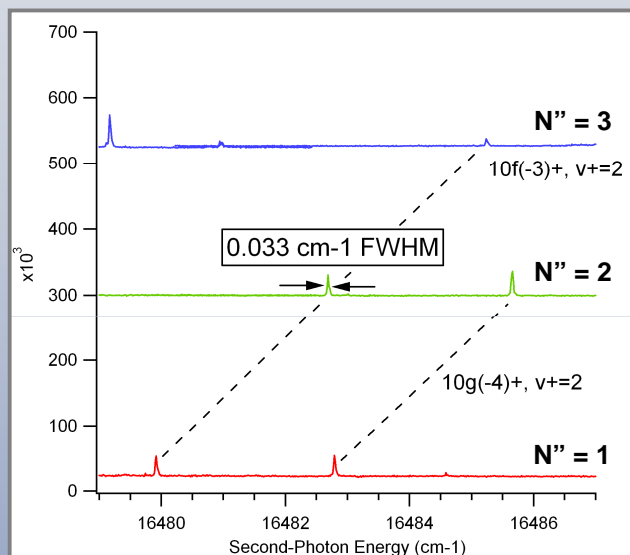
- Peter Bernath
- Mike Dulick LFT
- Bernard Pinchemel (Lille)
- Richard Barrow (Oxford) LFT
- Precila Ip BaF
- Steve Rice LFT
- David Baldwin CaO
- Jim Murphy MQDT
- Jon Berg
- Anthony Merer (UBC)
- Nicole Harris
- **Chris Gittins**
- Zygmunt Jakubek BaF
- Foss Friedman-Hill
- Leonid Kaledin
- Ed Murad (AFGL)
- Mike McCarthy
- Jon Bloch
- Jian Li (Tsinghua)
- Yaoming Liu (Tsinghua)
- Dave Moss
- Jason Clevenger CaCl
- Ma Hui (Tsinghua)
- Xing Jiang
- Dan Byun
- **Jeff Kay** Spectra + MDQT Fit*****
- Vladimir Petrovic
- **Christian Jungen** MQDT (Orsay)
- **Serhan Altunata** MQDT
- **Steve Coy** MQDT
- Bryan Wong MQDT
- **Kirill Kuyanov** CPmmW*****
- **Yan Zhou** CPmmW*****
- **Tony Colombo** CPmmW*****
- **Barratt Park** CPmmW*****
- \$\$\$ NSF

CaF Rydberg Papers

- spdf QD μ Matrix: Gittins, JCP **122** 184314 (2005)
- Ab Initio **R**-Matrix: Wong, JCP 124 014106 (2006)
- Shape Resonance, Altunata, JCP **124** 194302 (2006)
- Resonances: Kay, Mol. Phys. **105** 1661 (2007)
- fgh... ∞ Nonpenetrating: Kay, JCP **128** 194301 (2008)
- Polarization: Petrović, JCP **128** 014301 (2008)
- Stark Effect: Petrović, JCP 131 064301 (2009)
- spdf QD $\mu(R,E)$ Matrices: Kay, final preparation

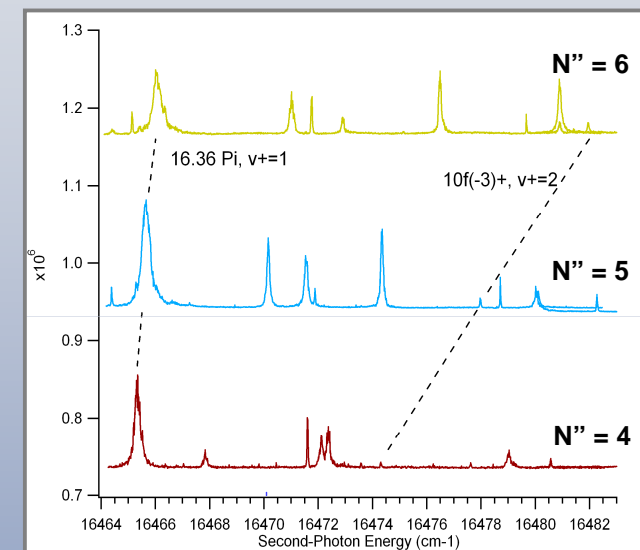


Improved Quality of Jeff Kay's Spectra: Resolution, Precision, Dynamic Range, Continuous Range of n^* and N



Resolution
widths, splittings

Data set specifics: resolution: 0.03 cm^{-1}

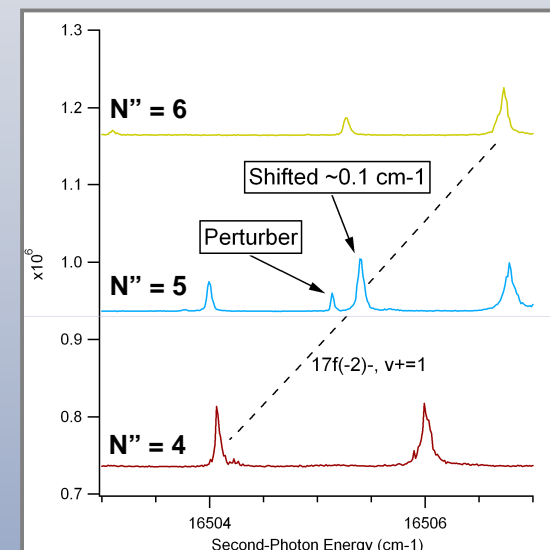


Dynamic Range
weak lines

calibration error: $<0.01 \text{ cm}^{-1}$ rms

rotational levels: $0 < N < 9$

energy range: $5 < n^* < 10$ ($v^+=0$), $16 < n^* < 21$ ($v^+=1$)



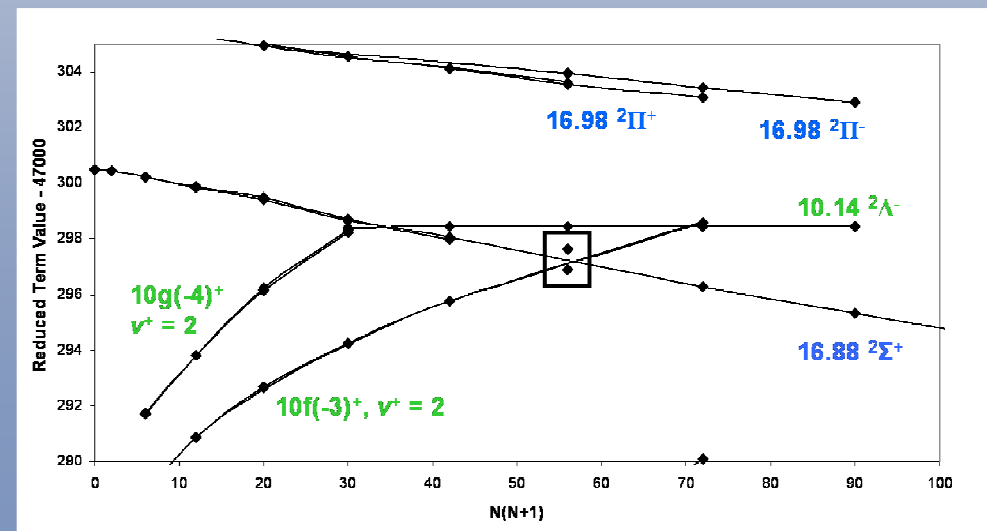
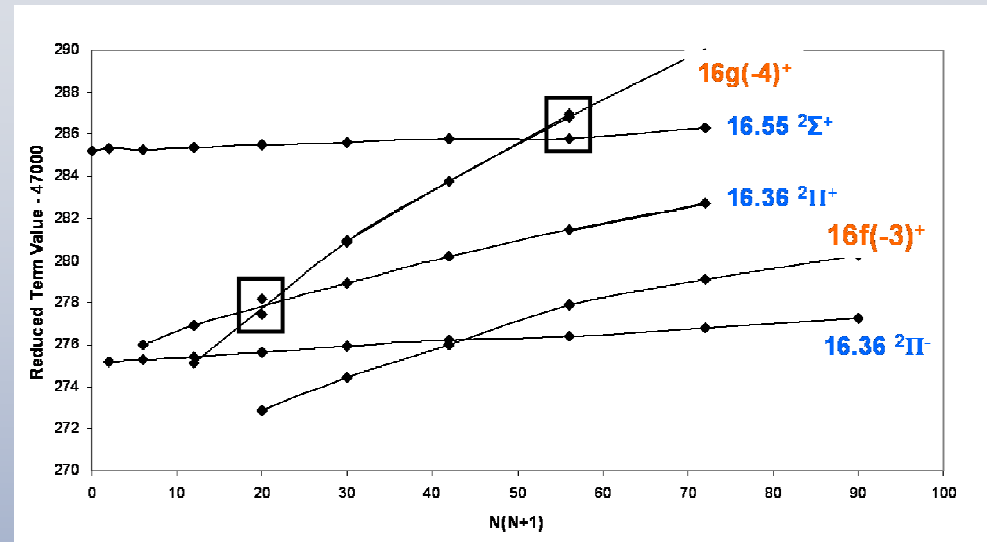
Precision
tiny level-shifts

A Zoology of Perturbations: $\Delta v = 0$ ℓ -Mixing and ℓ -Uncoupling; $\Delta v \neq 0$ due to $\mu(R)$ and $B(R)$

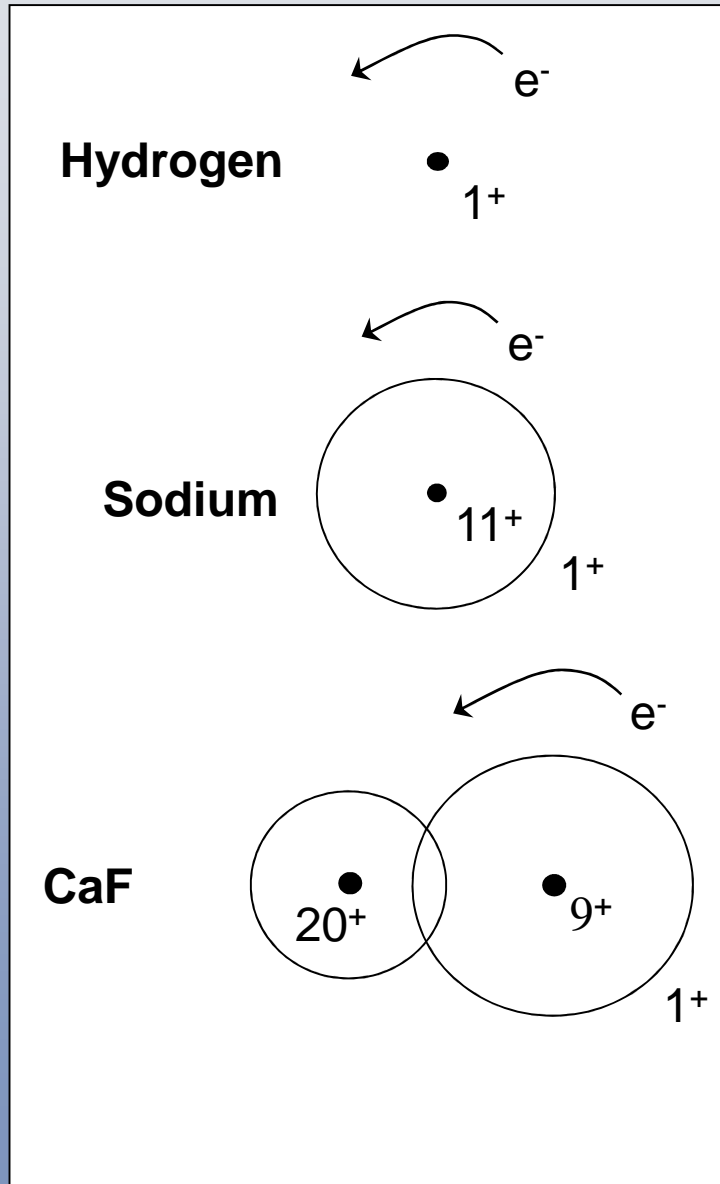
- Perturbations between penetrating and nonpenetrating states:

- $16g(-4)^+ \sim 16.36 \ ^2\Pi^+$
- $16g(-4)^+ \sim 16.55 \ ^2\Sigma^+$
- $17g(-4)^+ \sim 17.36 \ ^2\Pi^+$
- $17g(-4)^+ \sim 17.55 \ ^2\Sigma^+$
- $10f(-3)^+ \ v^+ = 2 \sim 16.88 \ ^2\Sigma^+$

- Matrix elements range from $<0.1 \text{ cm}^{-1}$ to $>1 \text{ cm}^{-1}$
- Perturbations sample core dipole, higher multipole moments, polarizability, and the R, E -derivatives of quantum defect matrix elements.



Multichannel Quantum Defect Theory (1)



$$E_{nl} = -\frac{\mathfrak{R}}{n^2}$$

$$n = | + 1, | + 2, \dots \infty$$

independent of ℓ

$$E_{nl} = -\frac{\mathfrak{R}}{\underbrace{(n - \delta_\ell)^2}_{n^*}}$$

$$n^*, n^* + 1, n^* + 2, \dots \infty$$

δ_ℓ is quantum defect

- independent of n
- dependent on ℓ

$\pi\delta_\ell$ is phase shift
(relative to H)

$$V_l(r) = -\frac{Z^{eff}(r)}{r} + \frac{l(l+1)}{2m_e r^2}$$

$$E_{nl\lambda} = -\frac{\mathfrak{R}}{(n - \mu_\alpha(R))^2}$$

Eigenquantum defect $\mu_\alpha(R)$

- R-dependent
- mixed ℓ

$$0 = |\mathbf{K} + \mathbf{P}(E)|$$

$$\downarrow \mathbf{K} = \tan \pi \boldsymbol{\mu}$$

$$\boldsymbol{\mu}(R, E) = \boldsymbol{\mu}(R_e^+) + \frac{d\boldsymbol{\mu}}{dR}(R - R_e^+) + \frac{d\boldsymbol{\mu}}{dE} E$$

$\mathbf{K}(R, E)$ reaction matrix

$\mathbf{P}(E)$ phase matrix

$\boldsymbol{\mu}(R, E)$ quantum defect matrix

\mathbf{H}^{eff} vs. \mathbf{K}, \mathbf{P}

Multichannel Quantum Defect Theory (2)

Eigenvalue Condition: $0 = \left| \mathbf{K}^{(N,p)} + \mathbf{P}(E)^{(N,p)} \right|$ N (rotation), Λ , and p (parity) are Good Quantum Numbers

Reaction Matrix Phase Matrix

Elements of
Non-Diagonal
Reaction Matrix:

$$K_{\ell, \ell'}^{(\Lambda)}(R) = \tan \pi \mu_{\ell, \ell'}^{(\Lambda)}(R)$$

Elements of
Diagonal
Phase Matrix:

$$P_{\ell_{v^+N^+}, \ell_{v^+N^+}}(E) = \tan \pi \nu_{v^+N^+}(E)$$

Effective Principal
Quantum Number

$$n^* = \left[\frac{\mathfrak{R}}{E_{v^+N^+} - E} \right]^{1/2} = \nu_{v^+N^+}(E)$$

Frame Transformations

fancy name for free stuff from $\mu^{(\Lambda,p)}(R)$

- Ion-core vibrational wavefunctions: $\chi_{v^+}(R)$

$$\int dR \chi_{v^+}(R) \mu_{\alpha\alpha'}^{(\Lambda,p)}(R) \chi_{v'^+}(R) = \mu_{\alpha v^+, \alpha' v'^+}^{(\Lambda,p)}$$

- Inter-series $\Delta v^+ \neq 0$ perturbations
- Vibrational autoionization

- Long-range coupling of Rydberg e⁻ angular momentum to angular momentum of molecular frame:

$$\dot{N} = \dot{N}^+ + \dot{l}$$

- $l_R = N^+ - N$
- N^+ is pattern-forming $[B^+ N^+(N^++1)]$, N is conserved
- Case (b) to (d) transformation of $\mu^{(\Lambda,p)}$: 3-j coefficients

$$\langle |N^+ N| | \Lambda N \rangle \langle | \Lambda N | | \mu^{(\Lambda,p)} | | ' \Lambda N \rangle \langle | ' \Lambda N | | ' N^+ ' N \rangle$$

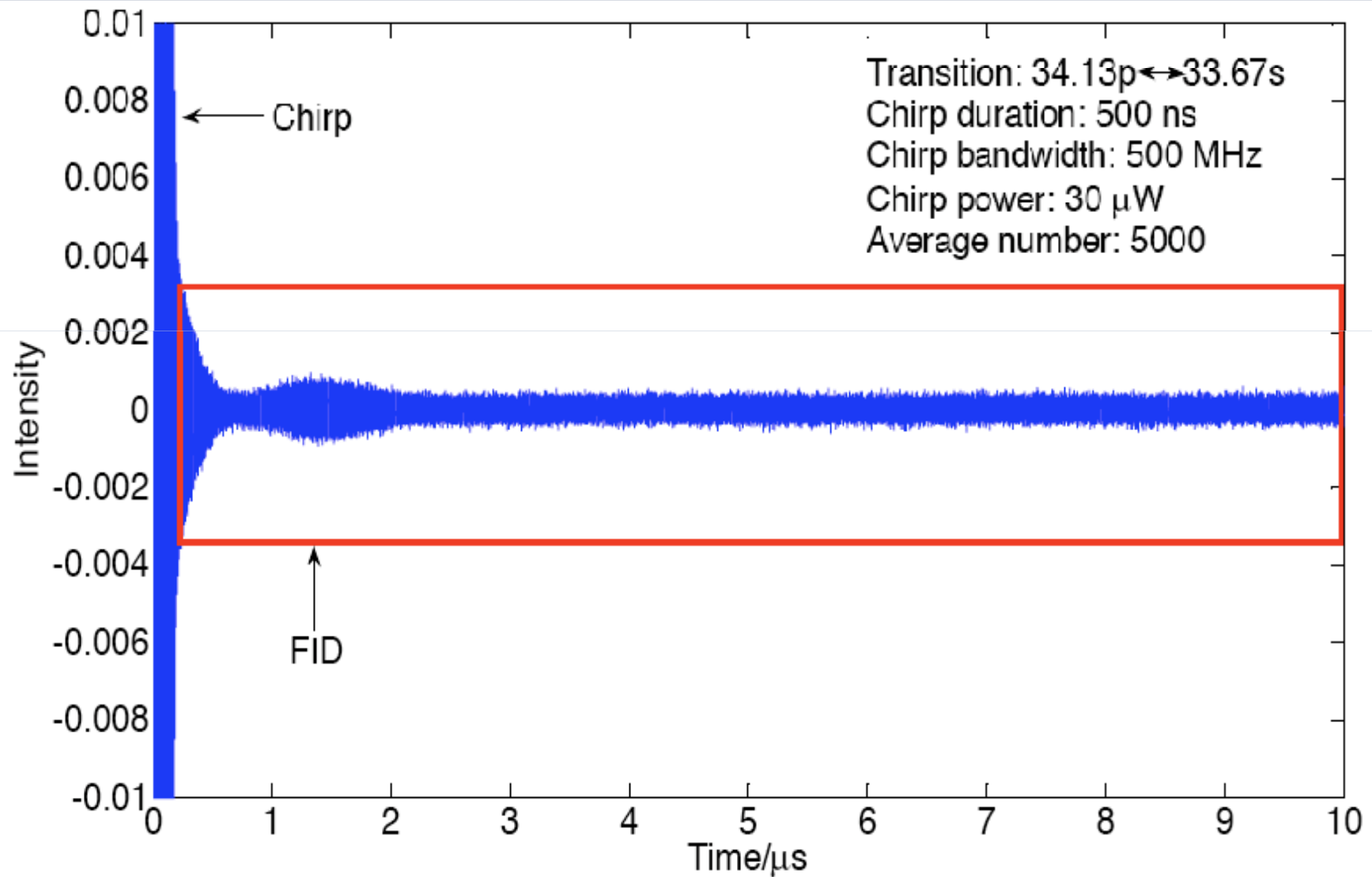
	$\mu(\mathbf{R}_e^+, \varepsilon=0)$	$\partial\mu/\partial\mathbf{R}$	$\partial\mu/\partial E$	$\partial^2\mu/\partial\mathbf{R}^2$	$\partial^2\mu/\partial E^2$	$\partial^2\mu/\partial E\partial\mathbf{R}$
ss Σ	0.3503(8)	-0.0720(73)	1.884(0)	1.147(25)	-54.27(24)	-4.31(30)
pp Σ	0.2224(10)	0.3860(11)	-0.793(70)	-1.132(33)	54.75(198)	-5.60(11)
dd Σ	-0.1350(2)	0.1095(45)	-0.084(30)	0.734(3)	33.56(15)	
ff Σ	-0.1100(8)	0.0930(105)		0.508(36)	-29.36(223)	7.12(43)
sp Σ	0.1553(1)	0.0217(17)	-0.198(23)	-0.579(10)		
pd Σ	0.04048(14)		-0.977(71)	0.178(44)		
df Σ	-0.0583(7)		0.117(62)	0.202(9)	6.15(245)	3.72(10)
sd Σ	-0.0369(19)	-0.1085(19)	-3.239(0)			
pf Σ		0.1121(59)	-0.138(114)			
sf Σ	-0.0466(31)	-0.0796(38)				
pp Π	-0.1758(6)	0.3348(16)	3.404(15)	-0.629(11)	6.11(79)	
dd Π	-0.1429(4)	0.3559(26)	-2.975(14)	0.503(13)	-4.16(43)	11.12(0)
ff Π	-0.0400(4)	0.0539(57)	-0.347(21)			
pd Π	0.1718(2)	-0.1395(16)	0.091(17)	0.425(9)	-62.89(68)	
df Π	-0.0148(6)				7.69(11)	
pf Π	0.0402(7)	0.0320(24)	-0.974(33)			
dd Δ	-0.1336(3)	0.2606(9)	-0.047(4)			
ff Δ	0.0235(3)	0.0891(19)				
df Δ	-0.0317(6)	-0.0339(12)				
ff Φ	0.0959(1)	0.2280(19)				

The **complete quantum defect matrix**, $\mu(E, R)$, for the s,p,d,f core-penetrating states. **All spectra, all dynamics...**

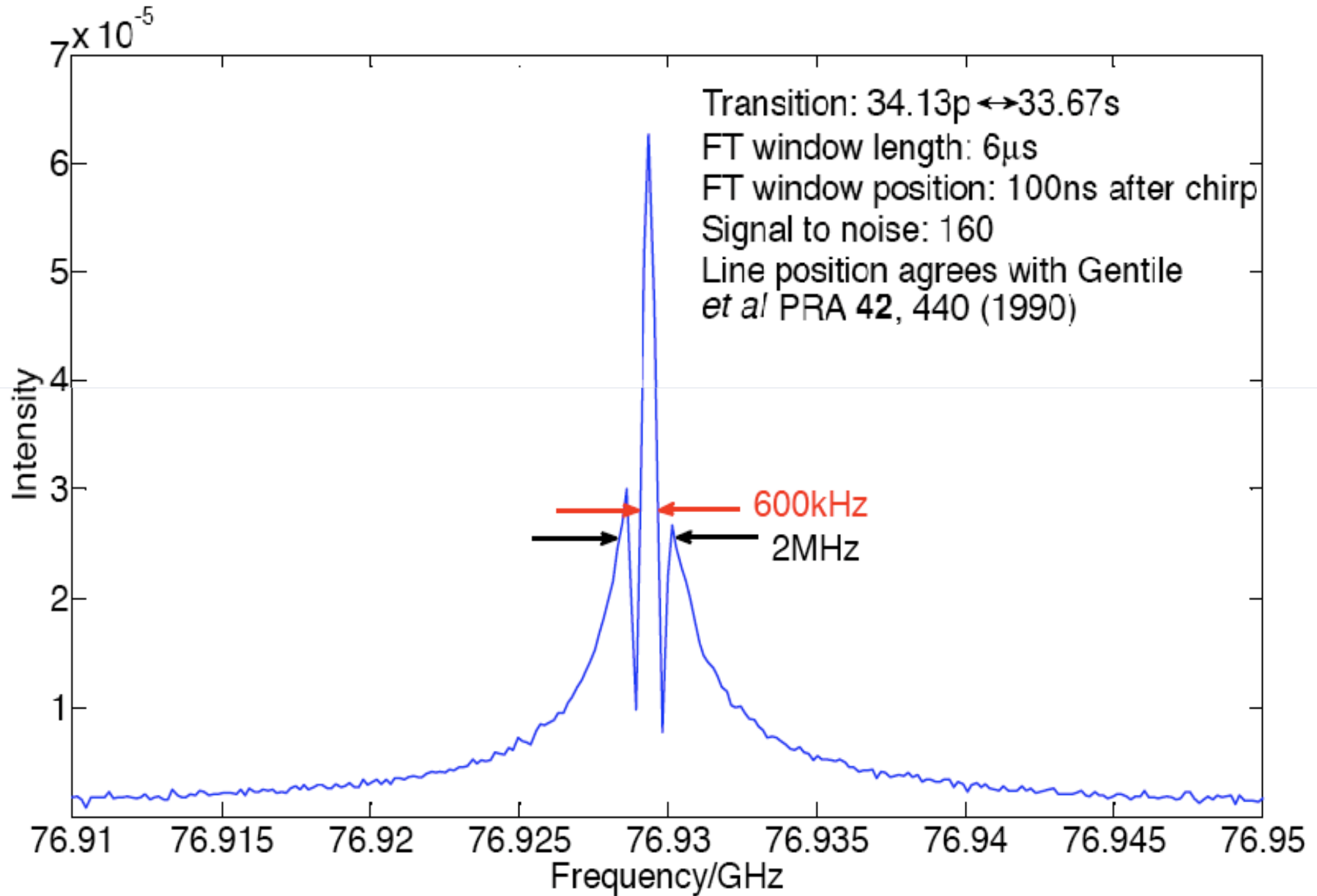
What Do These Matrix Elements Tell Us?

- Consequences of Not-Roundness
 - R-dependence
- Perturbations and Autoionization
 - Rates of dynamical processes
 - Where to look for specific class of process
- Unmet Challenge: Simple Reasons for Observed Values?
 - Relationships among μ , $d\mu/dR$, $d\mu/E$ elements?
 - Find a more compact and physical representation?
 - Unusual E dependence of one μ_α
 - a shape resonance

Chirp and FID



CPmmW Lineshape: 5000 Shots



Semi-Classical Resonances

Any two intramolecular motions may be tuned to have the same period

Kepler Period $T_{Kepler}(n^*) = \frac{h}{E_{n^*+1/2} - E_{n^*-1/2}} = \frac{h}{2hc\mathcal{R}/n^{*3}} \propto n^{*+3}$

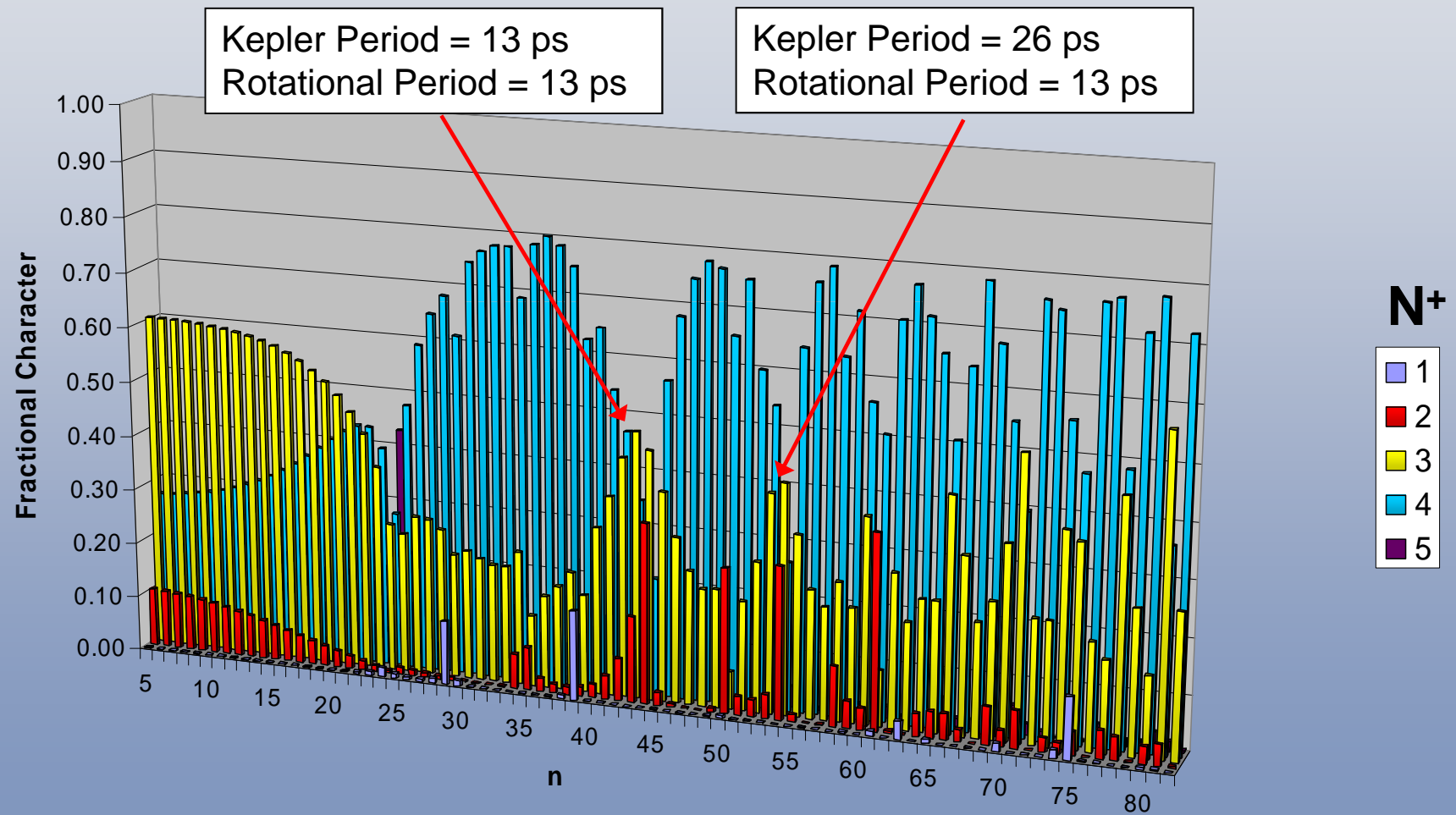
Vibrational Period $T_{vib}(v) = \frac{h}{(E_{v+1} - E_{v-1})/2} = \frac{h}{hc\omega_e} \propto v^0$

Rotational Period $T_{rot}(N) = \frac{h}{(E_{N+1} - E_{N-1})/2} = \frac{h}{hcB[2N+1]} \propto N^{-1}$

Multipole Precession $T_{\mu,Q}(\lambda) = \frac{h}{(E_{\lambda+1} - E_{\lambda-1})/2} \propto \frac{1}{(\mu^2 - Q)\lambda} \propto \lambda^{-1}$

At a selected **resonance**, energy flows rapidly between two *selected* modes. Away from resonance, the two modes are *dynamically decoupled*.

Stroboscopic Effects

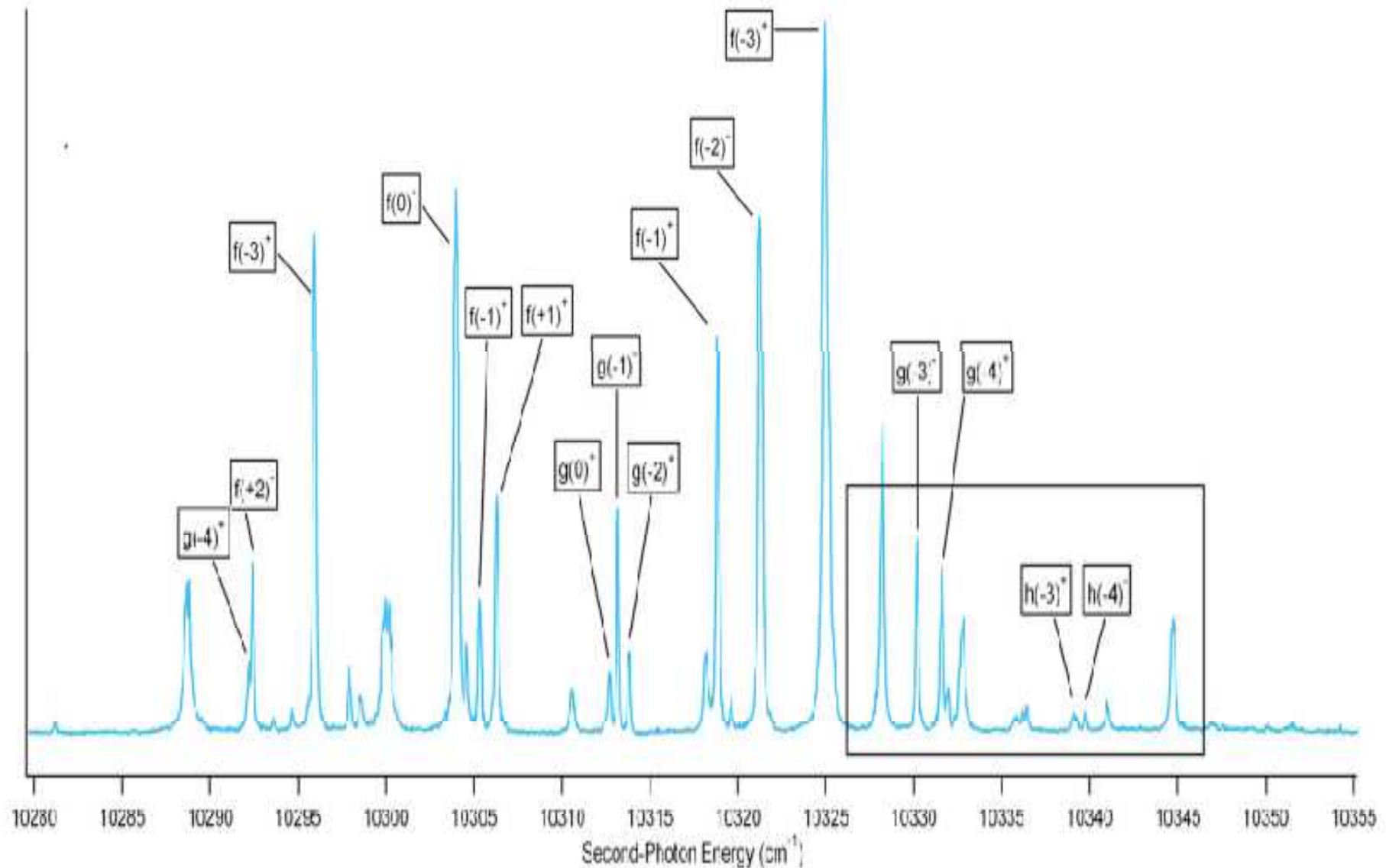


'p' Π Series; $N = 3$

Long Range Model

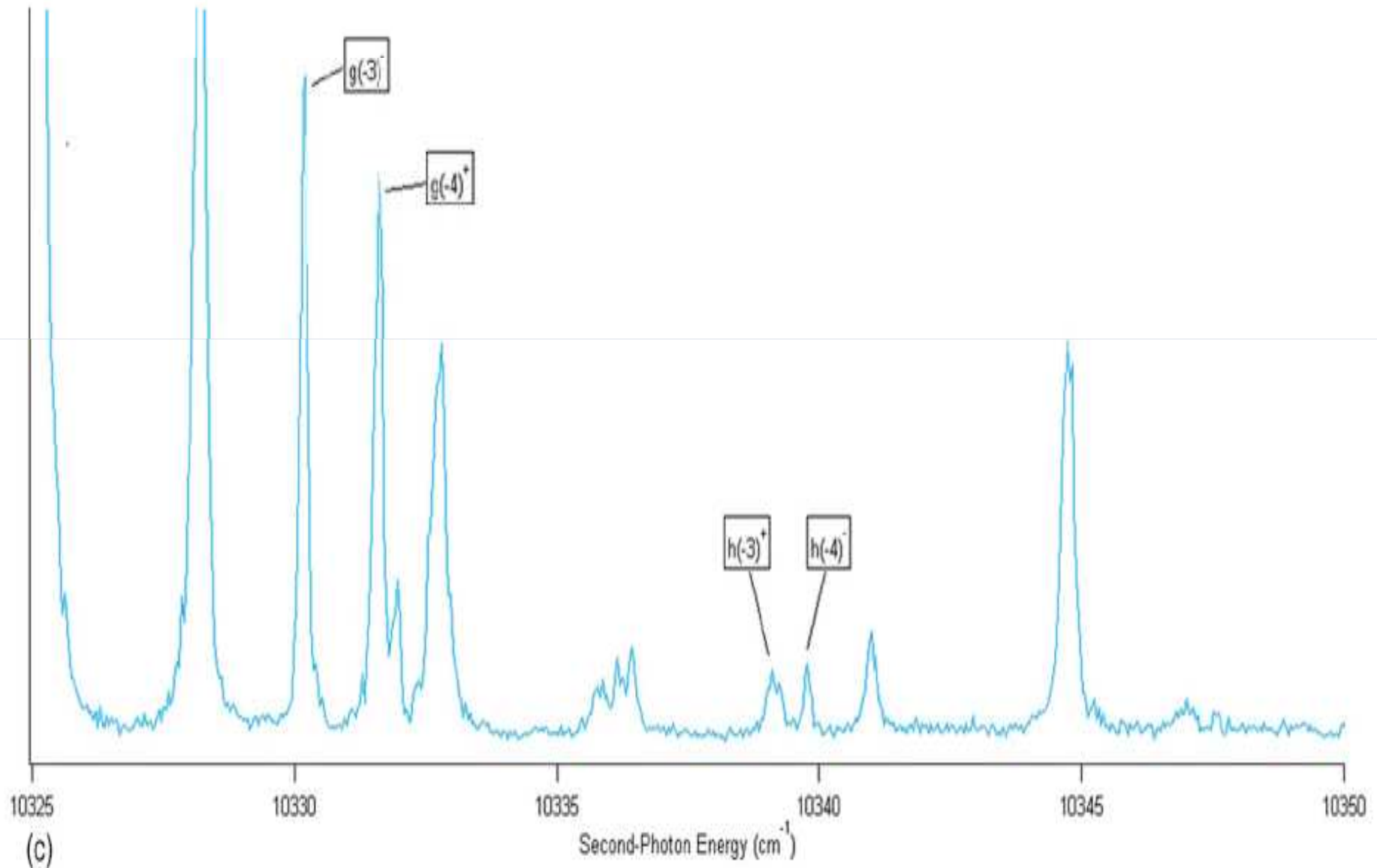
- Ion-Core Electronic Structure
 - μ , \mathbf{Q} , \mathbf{O} , \mathbf{H} moments
 - α , γ dipole polarizability components
 - Fancy Computer-Automated Algebra
 - Observed splittings near integer n^* (need very high resolution)
- ↓
- Ion-Core Multipole Moments and Polarizability
 - Describes All Nonpenetrating ℓ
 - $3 < \ell < n-1$

Nonpenetrating States Live Near Integer n^*

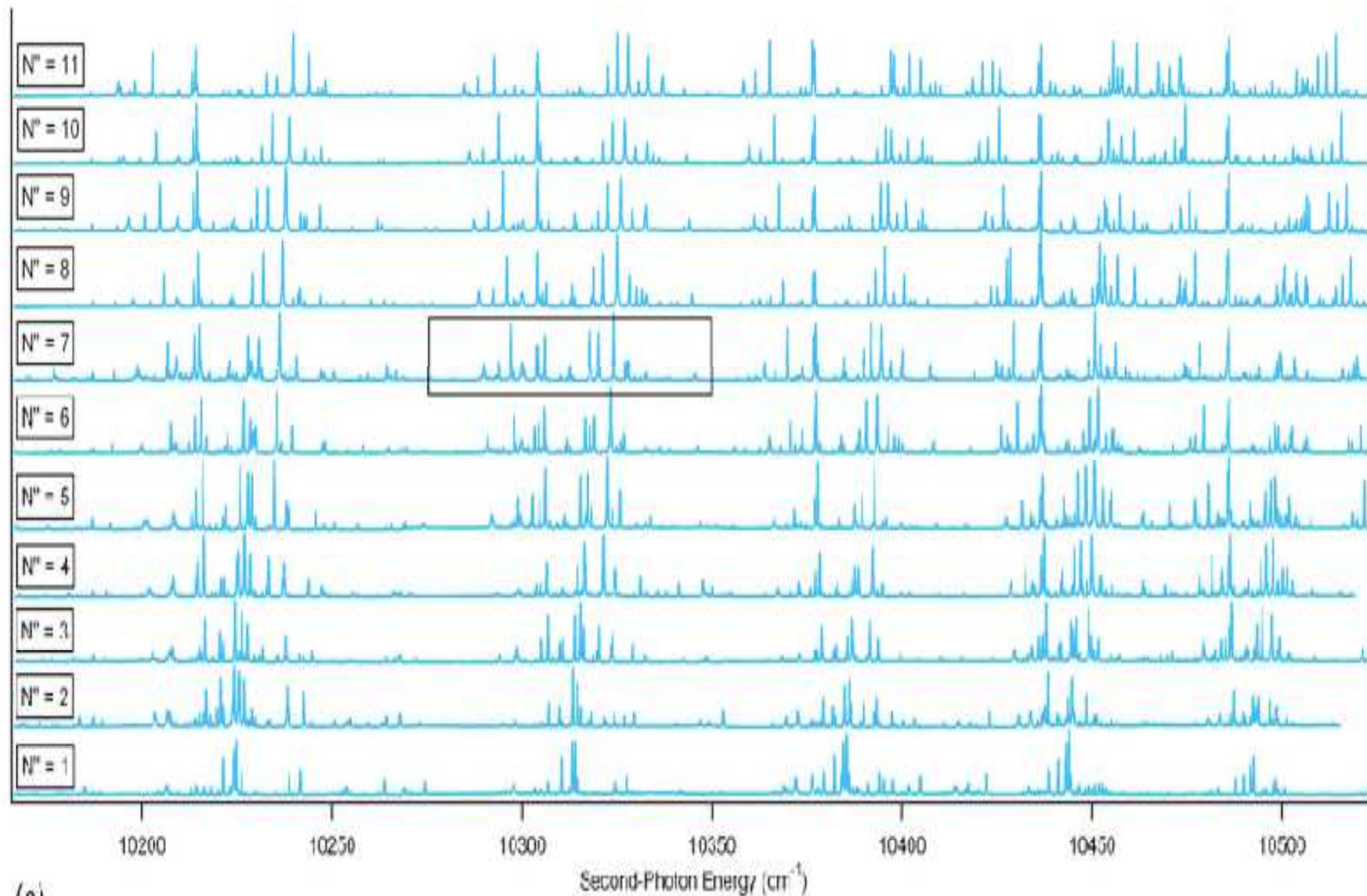


(h)

High Resolution Detective Work Required



Nonpenetrating States: Stacked Plot for N , N^+ Assignment



(a)

Pattern-Forming Quantum Number

$$\begin{aligned} \mathbf{H}^{ROT} &= B(\mathbf{N} - \ell)^2 \\ &= B \left[N(N+1) - \lambda^2 + \ell(\ell+1) - \lambda^2 + \underbrace{(\mathbf{N}^+ \ell^- + \mathbf{N}^- \ell^+)}_{\ell\text{-Uncoupling}} \right] \end{aligned}$$

Case (b)

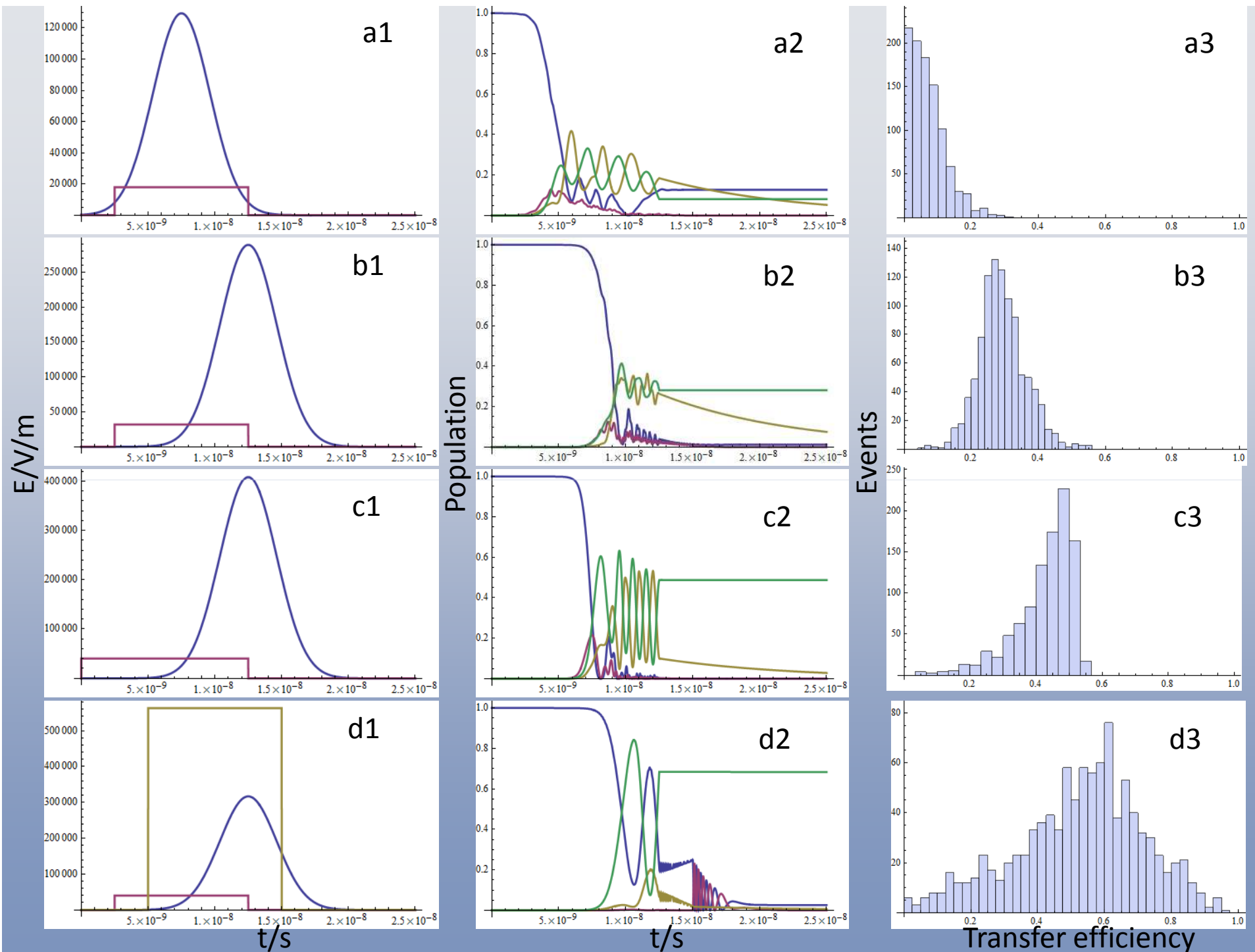
$$\begin{aligned} \mathbf{H}^{ROT} &= B(\mathbf{N}^+)^2 = BN^+(N^+ + 1) \\ N^+ &= N - \ell_R \quad (\ell_R \text{ is projection of } l \text{ on } \mathbf{N}^+) \\ \mathbf{H}^{ROT} &= B(N - \ell_R)(N - \ell_R + 1) \\ &= B \left[N(N+1) - \underbrace{2\ell_R N}_{\text{Anomalous}} + \ell_R^2 - \ell_R \right] \\ &\quad B_{eff} \end{aligned}$$

Case (d)

N Determined From Combination Differences

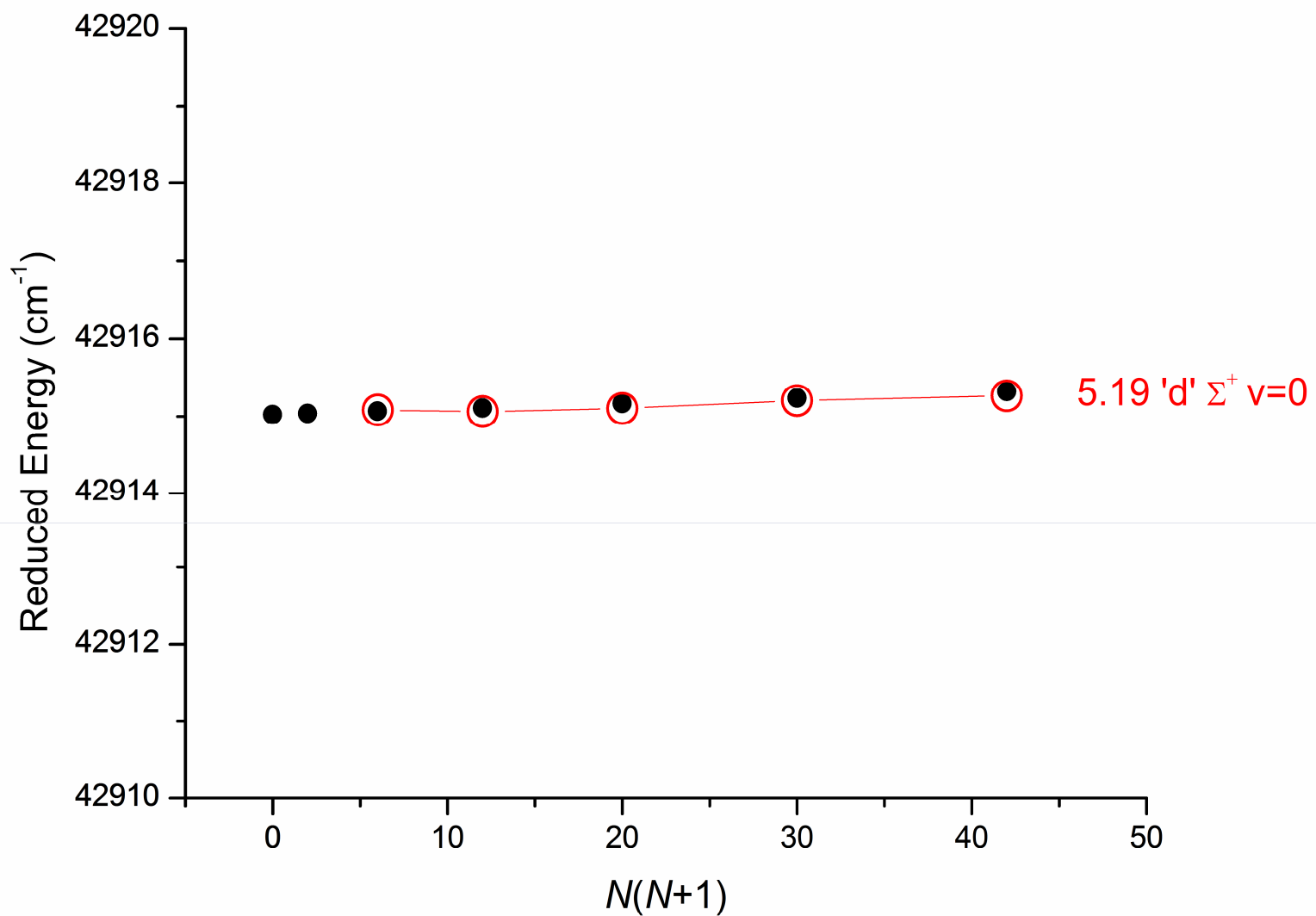
Plot $E^{ROT} - BN(N+1)$ vs. N

Slope is $-2B\ell_R$; Determines N^+

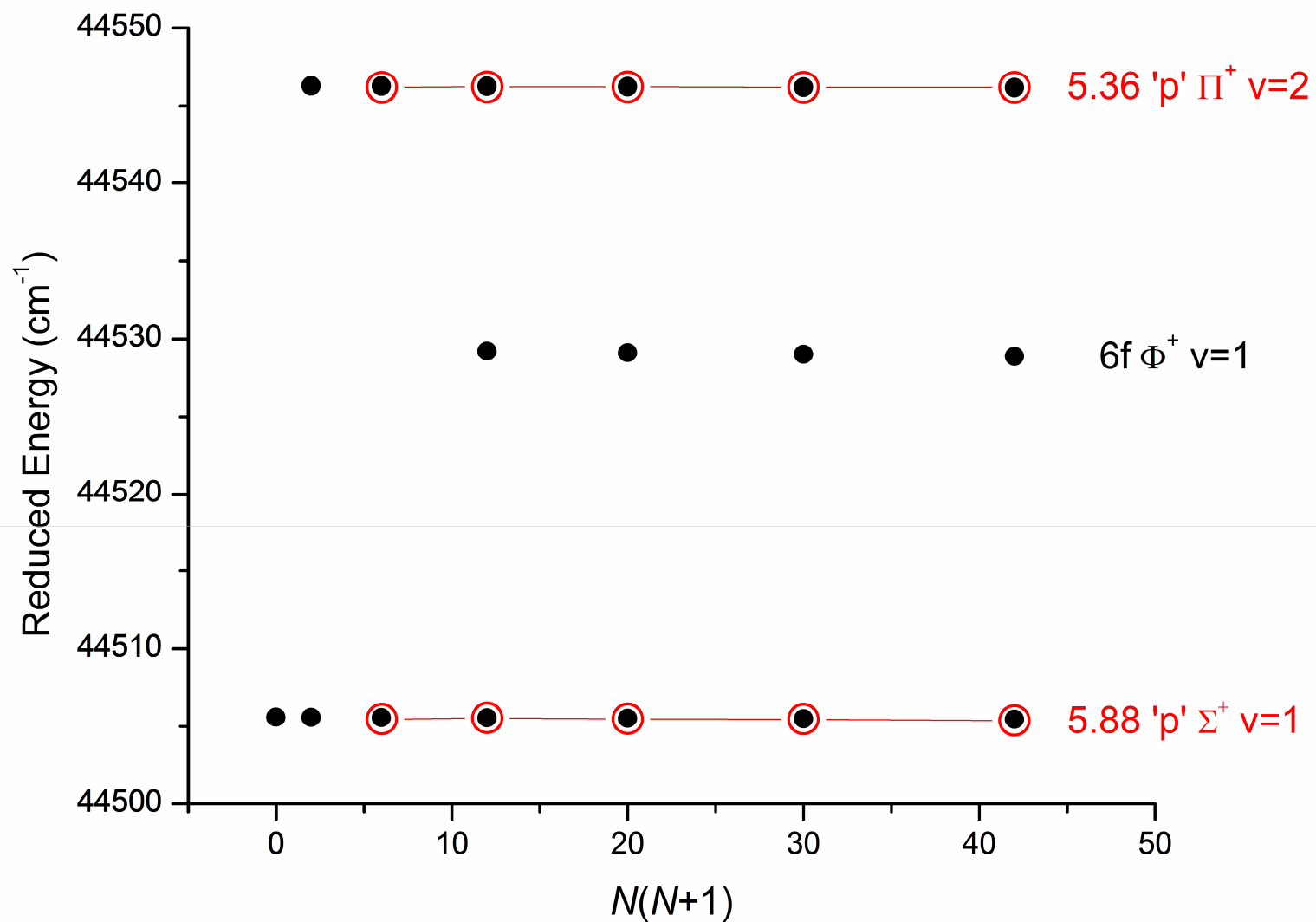


Pure Electronic Spectroscopy

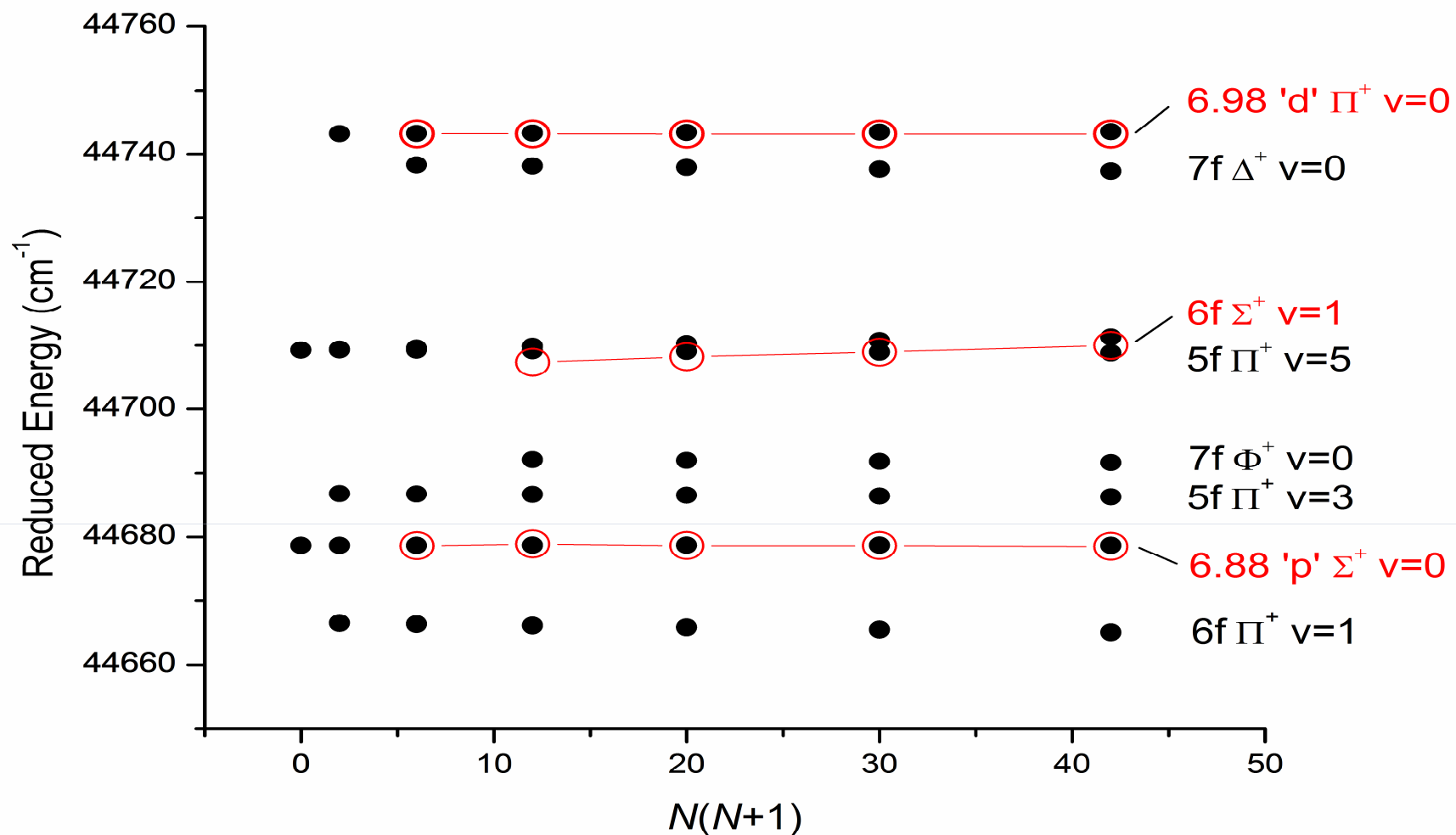
- Transitions between core-nonpenetrating states
- Integer n^*
- Intra-core dynamical processes turned off
- ng to $(n+1)h$ transitions
 - 1000 Debye transition moment
 - No torque, no impulse: $\Delta v^+ = 0$, $\Delta J^+ = 0$
Need very high resolution to sample ion-core multipole moments and polarizability
- Long-range model



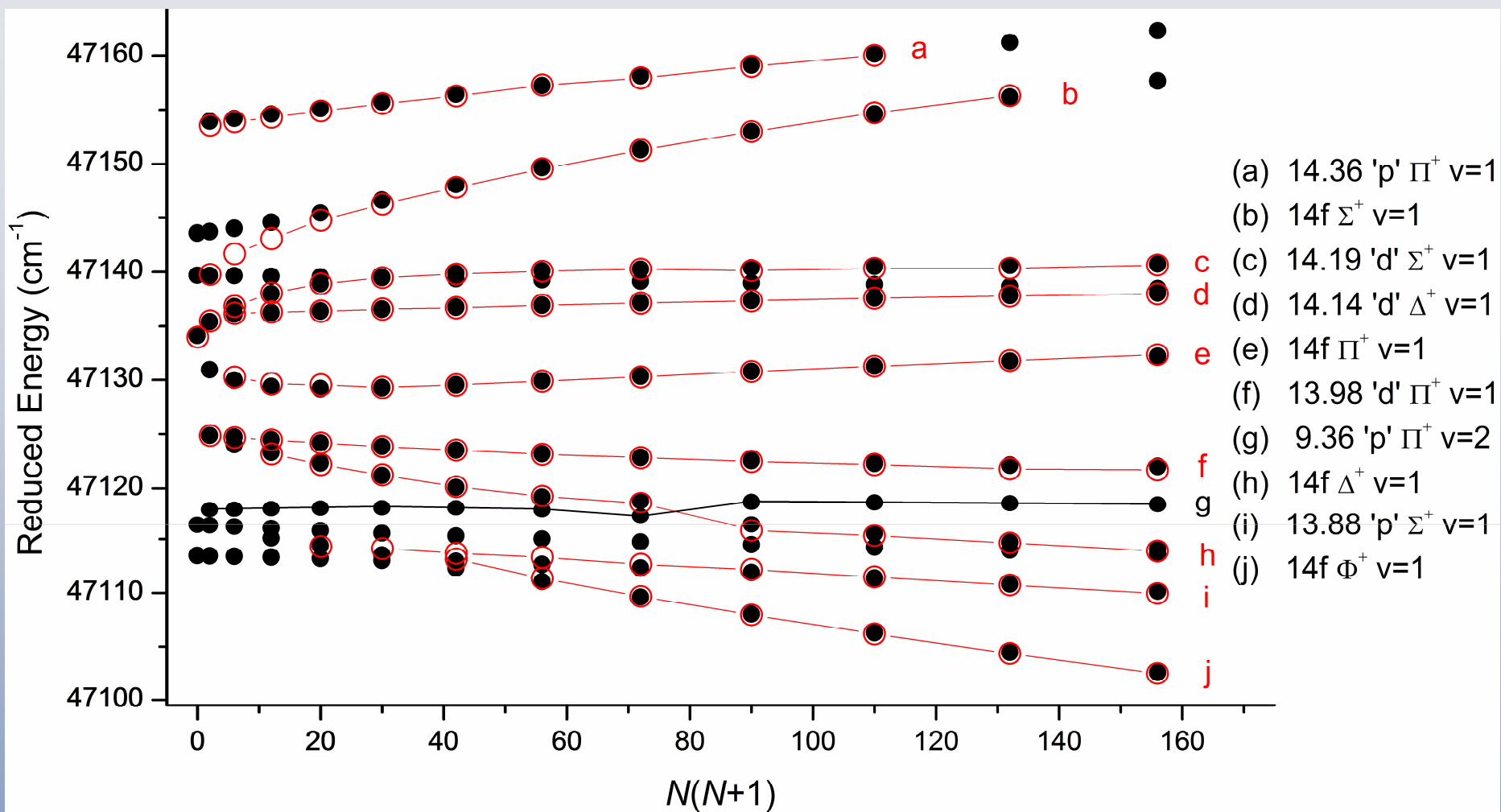
Quality of fit near $n^* = 5.0$, where vibronic states tend to be well-separated



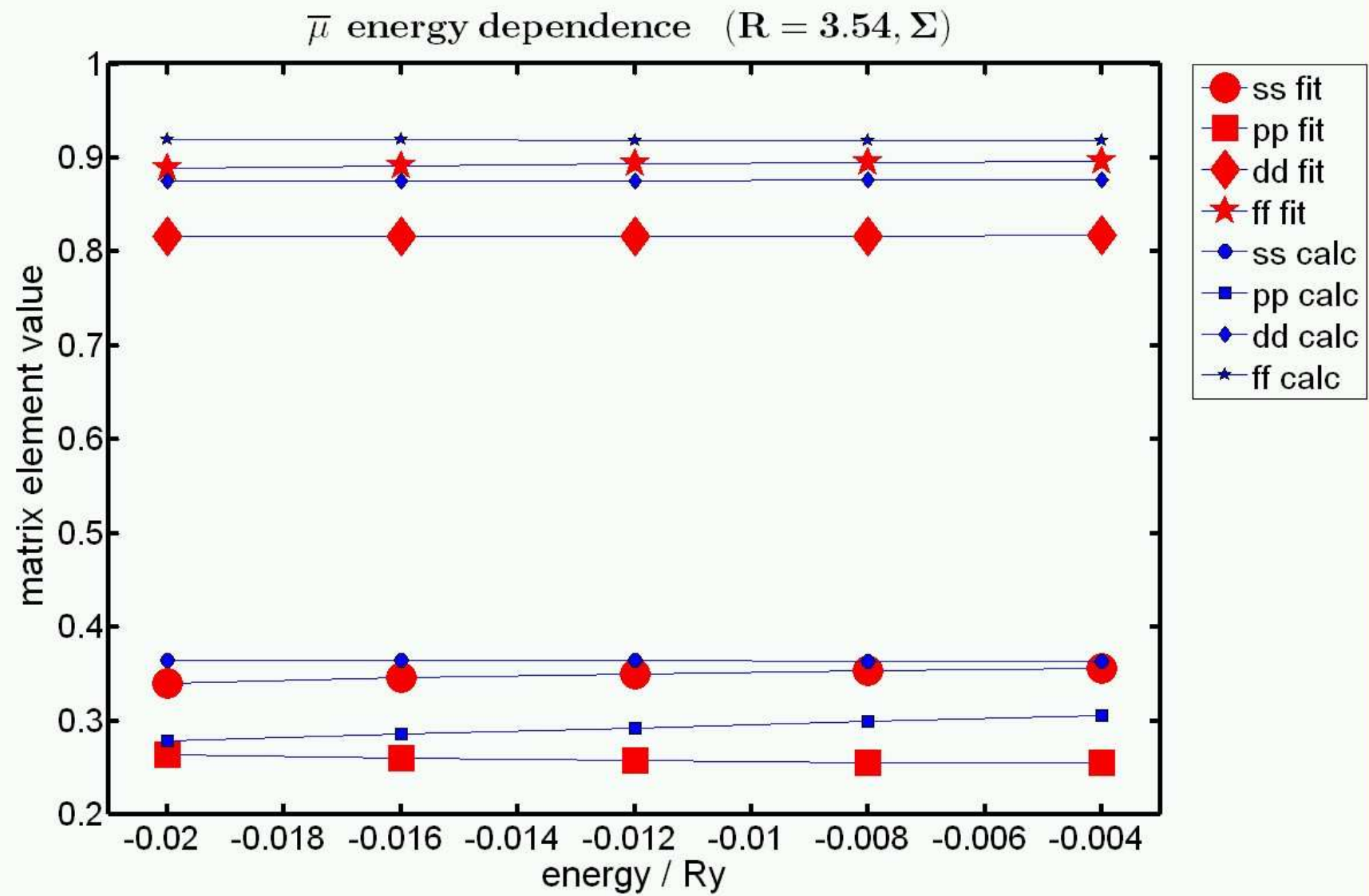
Quality of fit for vibrationally-excited levels with low n^* .



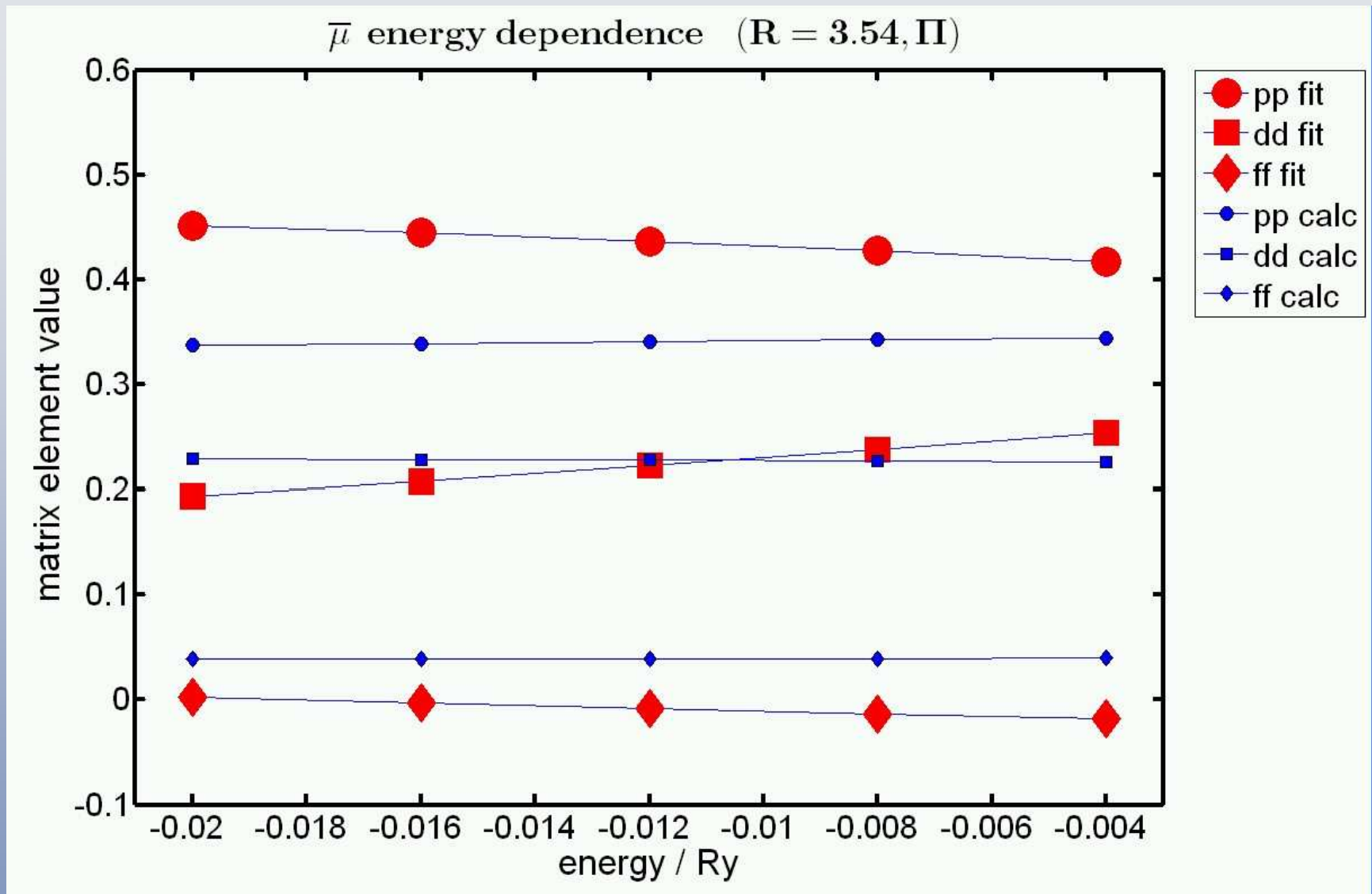
Quality of fit in the vicinity of $n^* = 7.0$. Vibronic states at this energy are interleaved. Here, the classical period of electronic motion (proportional to n^{*3}) is approximately equal to the classical period of vibrational motion. Vibronic perturbations are frequent.



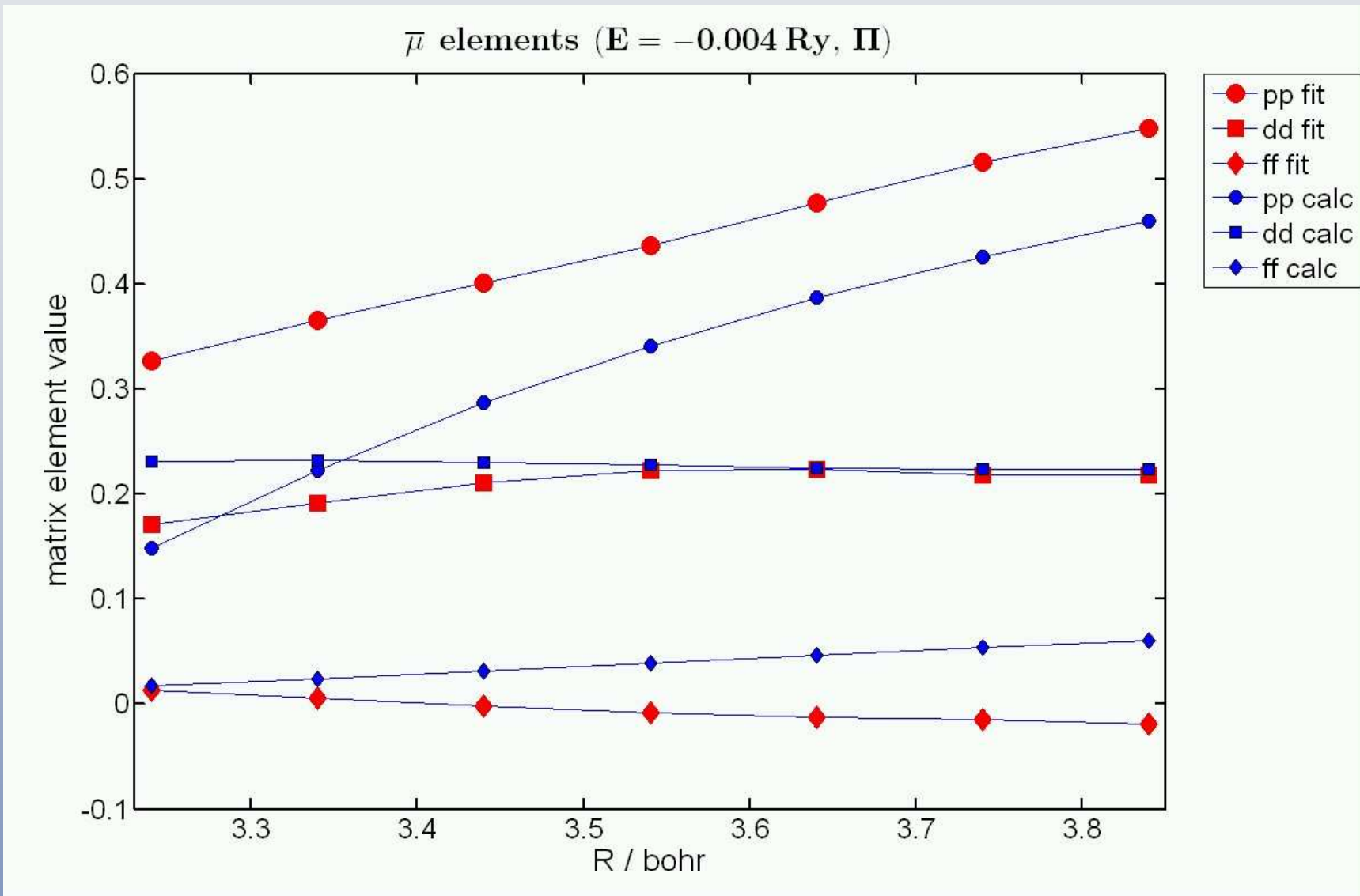
Quality of fit in the vicinity of $n^* = 14.0$. At this energy, the electronic energy level spacing is much smaller than the vibrational spacing, but still larger than the rotational spacing of the ion core energy levels. Vibronic perturbations are uncommon, but rotational (inhomogeneous) perturbations become increasingly frequent. An avoided crossing can be seen between 14f Δ^+ v=1 and 9.36 'p' Π^+ v=2.



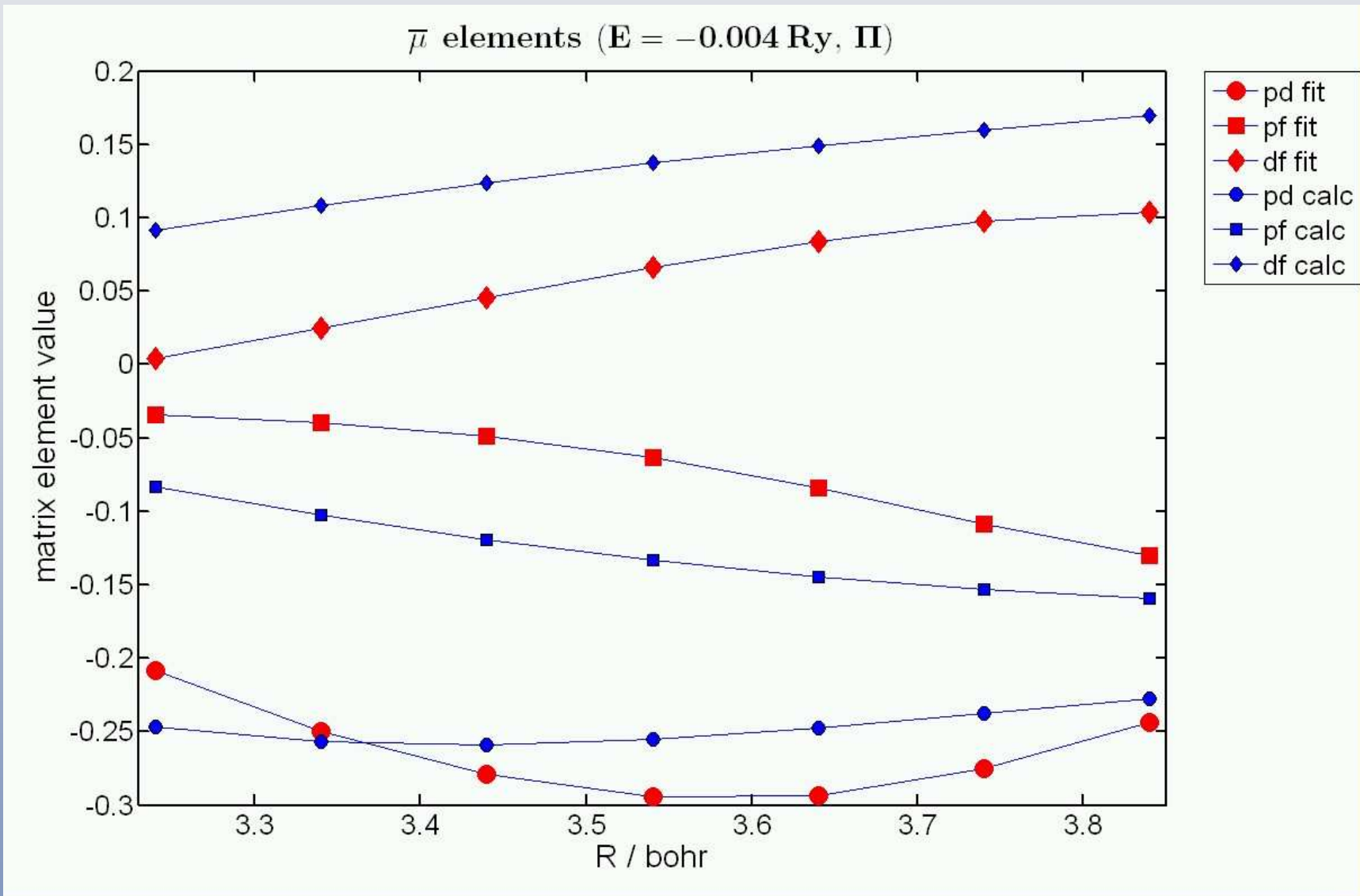
Fitted and computed quantum defects for Σ symmetry, at $R = R_e^+ = 3.54 a_0$.



Quantum defects for Π symmetry, at $R = R_e^+ = 3.54 a_0$.



Quantum defects for Π symmetry, at $E = -0.004 \text{ Ry}$, diagonal elements.



Quantum defects for Π symmetry, at $E = -0.004 \text{ Ry}$, off-diagonal elements.

CaF: The “Alkali Atom of Diatomic Molecules” with a Highly Polar Ion-Core

Multipole Moments (atomic units):

	μ	Q
CaF+	0	11.3
NO+	0	~ 0.74

Center of Charge
Coordinates

	μ	Q
CaF+	3.52	8.96
NO+	0.15	0.74

Center of Mass
Coordinates

CaF⁺ (center of mass) dipole moment: **8.9 Debye**

CaF $v=0$ to $v^+=0$ Ionization Potential: **$\sim 47,000 \text{ cm}^{-1}$**

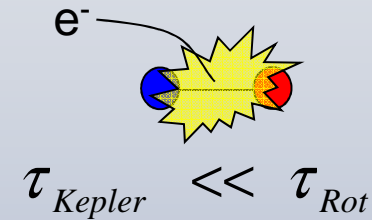
CaF $v=0$ to Ca(¹S) + F(²P) Dissociation Energy: **$\sim 44,200 \text{ cm}^{-1}$**

($n^* \approx 6$)

Separated-Atom Excited States: Ca 4s4p ³P at **$> 15,000 \text{ cm}^{-1}$**

Classical Mechanism

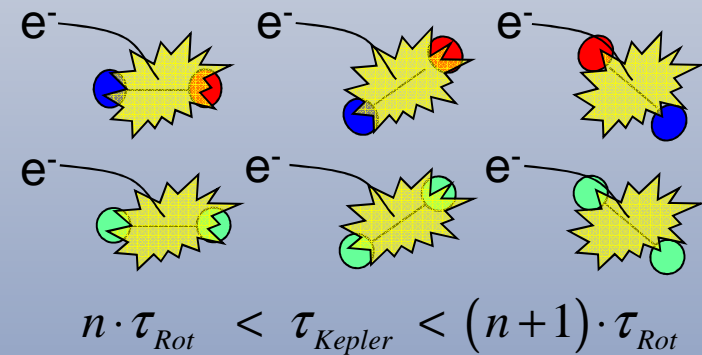
Low n^* : Core essentially **stationary**



High n^* but **not resonant**:

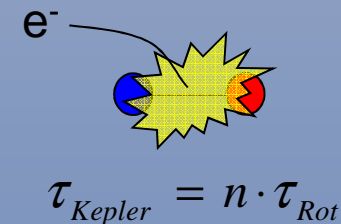
Odd-rank electrostatic interactions
average toward zero

Even-rank interactions *persist*

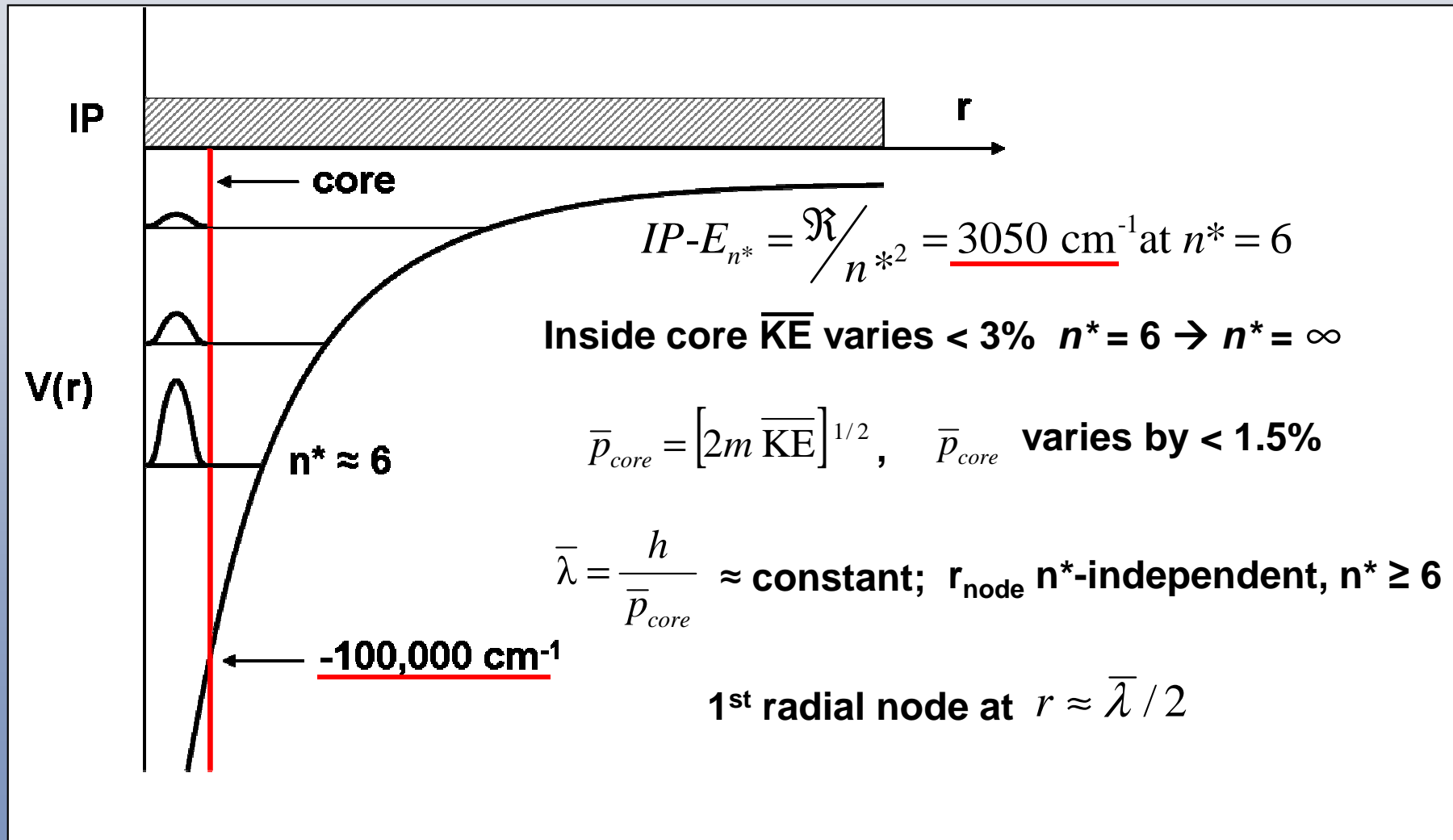


High n^* but **resonant**:

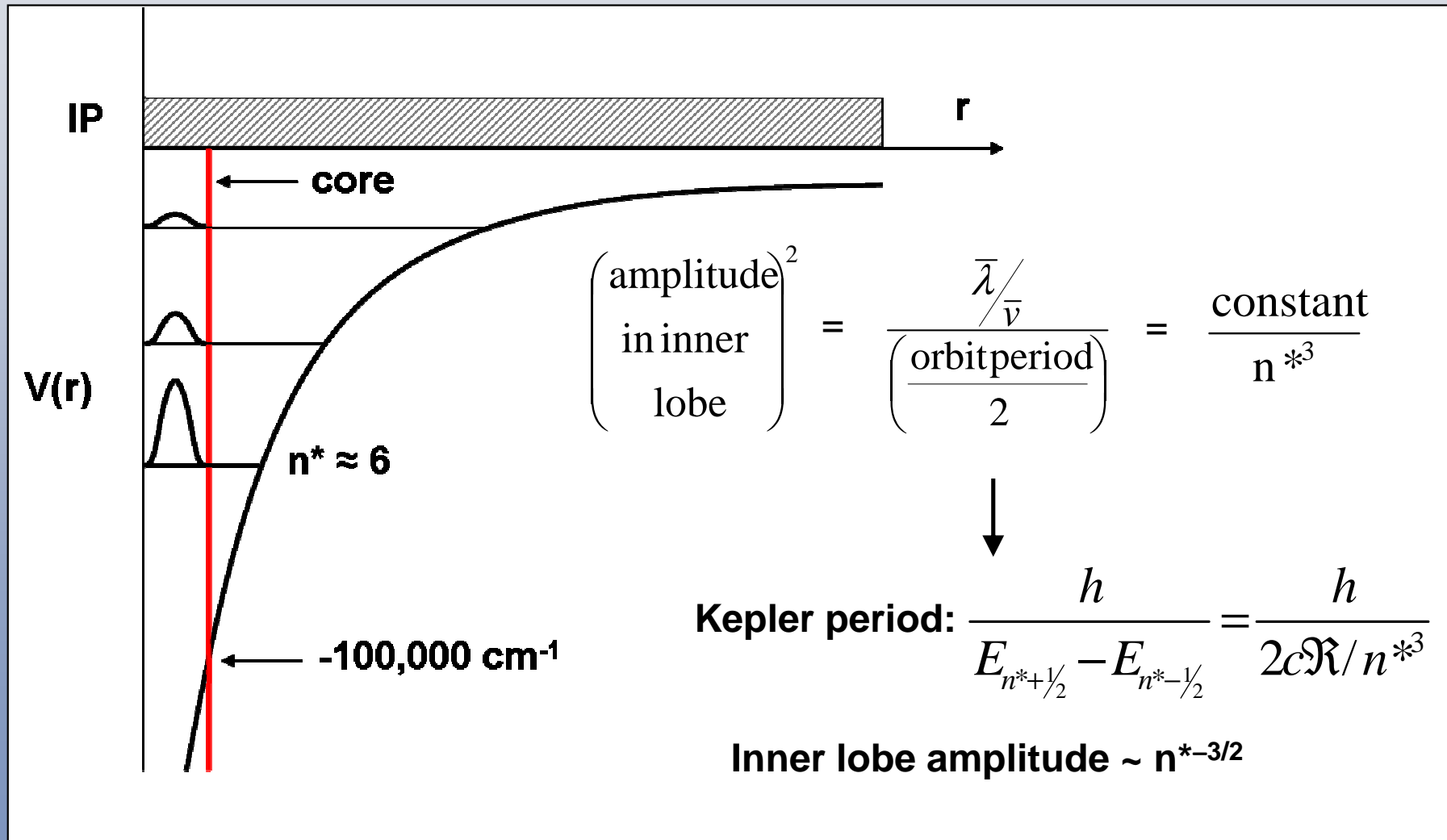
Core *appears stationary*



Physical Basis for n^{*-3} Scaling (1)



Physical Basis for n^{*-3} Scaling (2)



Mulliken's Rule

“Ontogeny recapitulates phylogeny” (E. Haeckel, ~1900).

The growth of the organism from a single cell to adult mirrors the evolutionary development of the species.

The innermost lobes of a Rydberg orbital remain invariant (shapes, positions of nodes) for all members of a Rydberg series, aside from an $n^{*-3/2}$ amplitude scale factor.

The low- n^* terminus state of a Rydberg series is *explained* by LCAO-MO (bonding/antibonding) or LFT (shielding).

Most dynamics is *encoded* in the innermost lobe.

Basis for n^* -*scaling* of everything in Rydberg-land.

Franck-Condon Factors

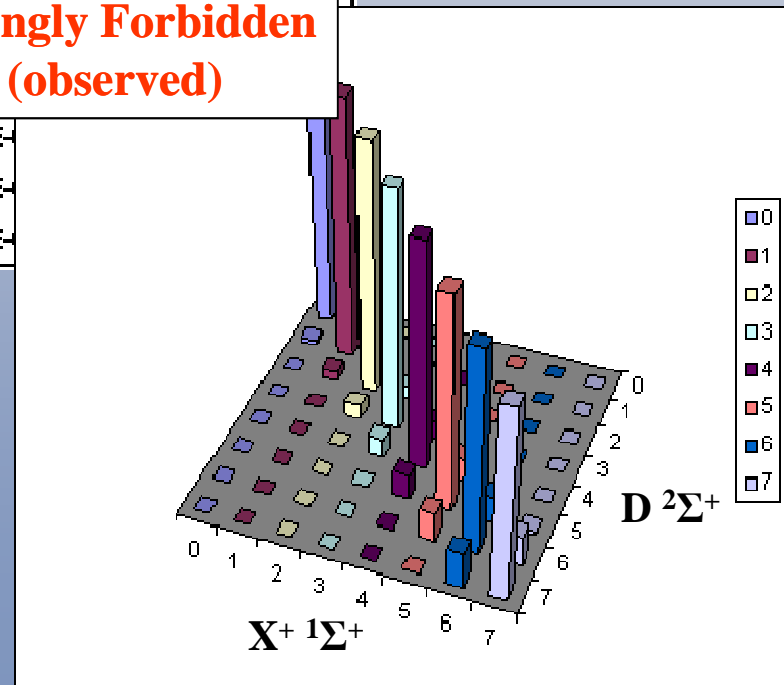
		$X^+ 1\Sigma^+$							
		$v^+ \rightarrow$							
		0	1	2	3	4	5	6	7
$D 2\Sigma^+$	0	9.83E-01	1.68E-02	2.66E-05	4.96E-06	7.66E-07	5.51E-08	3.20E-09	1.63E-10
	1	7.65E-02	9.40E-01	3.46E-02	9.61E-05	1.90E-06	3.83E-08	3.32E-07	2.23E-08
	2	3.76E-04	3.32E-02	9.13E-01	5.32E-02	2.30E-04	4.52E-05	4.55E-05	4.47E-06
V	3	1.13E-03	4.99E-02	8.76E-01	7.25E-02	7.97E-04	7.97E-04	7.97E-04	7.97E-04
	4	4.43E-06	2.46E-03	1.25E-01	7.97E-02	7.97E-02	7.97E-02	7.97E-02	7.97E-02
	5	5.35E-07	1.25E-04	1.70E-01	7.97E-02	7.97E-02	7.97E-02	7.97E-02	7.97E-02
6	3.40E-10	1.12E-08	1.70E-01	7.97E-02	7.97E-02	7.97E-02	7.97E-02	7.97E-02	
7	1.13E-10	1.12E-08	1.70E-01	7.97E-02	7.97E-02	7.97E-02	7.97E-02	7.97E-02	

Strongly Allowed
(observed)

Weakly Allowed
(observed)

Forbidden
(observed)

Strongly Forbidden
(observed)



FID Contains Ca 34.13p-33.67s: Polarized by 500 MHz Chirp

